# Future High-Resolution and High-Cadence Observations for Unraveling Small-Scale Explosive Solar Features

**Alphonse C. Sterling** [1,*], **Ronald L. Moore** [2,1], **Navdeep K. Panesar**[3,4], **Tanmoy Samanta**[5], **Sanjiv K. Tiwari**[3,4] **and Sabrina L. Savage** [1]

[1] *NASA, Marshall Space Flight Center, Huntsville, AL 35812, USA*
[2] *Center for Space Plasma and Aeronomic Research, University of Alabama in Huntsville, Huntsville, AL 35805, USA*
[3] *Lockheed Martin Solar and Astrophysics Laboratory, 3251 Hanover Street Building 252, Palo Alto, CA 94304, USA*
[4] *Bay Area Environmental Research Institute, NASA Research Park, Moffett Field, CA 94035, USA*
[5] *Indian Institute of Astrophysics, Koramangala, Bangalore 560034, India*

Correspondence*:
A. C. Sterling
alphonse.sterling@nasa.gov

## ABSTRACT

Solar coronal jets are frequently occurring collimated ejections of solar plasma, originating from magnetically mixed polarity locations on the Sun of size scale comparable to that of a supergranule. Many, if not most, coronal jets are produced by eruptions of small-scale filaments, or minifilaments, whose magnetic field reconnects both with itself and also with surrounding coronal field. There is evidence that minifilament eruptions are a scaled-down version of typical filament eruptions that produce solar flares and coronal mass ejections (CMEs). Moreover, the magnetic processes building up to and triggering minifilament eruptions, which is often flux cancelation, might similarly build up and trigger the larger filaments to erupt. Thus, detailed study of coronal jets will inform us of the physics leading to, triggering, and driving the larger eruptions. Additionally, such studies potentially can inform us of smaller-scale coronal-jet-like features, such as jetlets and perhaps some spicules, that might work the same way as coronal jets. We propose a high-resolution ($\sim$0.″1 pixels), high-cadence ($\sim$5 seconds) EUV-solar-imaging mission for the upcoming decades, that would be dedicated to observations of features of the coronal-jet size scale, and smaller-scale solar features produced by similar physics. Such a mission could provide invaluable insight into the operation of larger features such as CMEs that produce significant Space Weather disturbances, and also smaller-scale features that could be important for coronal heating, solar wind acceleration, and heliospheric features such as the magnetic switchbacks that are frequently observed in the solar wind.

**Keywords: Solar filament eruptions, solar corona, solar x-ray emission, solar extreme ultraviolet emission, solar coronal jets, solar magnetic activity**

## 1 INTRODUCTION

Solar coronal jets are transient phenomena that originate near the solar surface and extend into the corona in the form of long and narrow spires. They are visible at soft X-ray (SXR) and EUV wavelengths, and occur in coronal holes, quiet Sun, and the periphery of active regions. While there were some scattered earlier observations, coronal jets were first observed in detail in SXRs with the *Yohkoh* satellite (Shibata et al., 1992), and they have since been observed with several instruments in different wavelengths. (Surges, which traditionally have been observed in the chromosphere, share some properties with coronal jets, and in some cases accompany coronal jets; e.g., Canfield et al. 1996; Moore et al. 2010, 2013; Sterling et al. 2016.) In coronal images, coronal jets consist of a spire that emanates from a bright base region and extends into the corona. From a study of SXR coronal jets in polar coronal holes (Savcheva et al., 2007), coronal jets live for tens of minutes, and have an occurrence rate of about 60/day in the two polar coronal holes, which translates to about one per hour in a given polar coronal hole. That same study reported that the coronal-jet spires reach $\sim$50,000 km, and have widths $\sim$10,000 km. Coronal jets seem to have two speeds, or two components of different speeds; a slower speed of $\sim$200 km s$^{-1}$, which is close to the local sound speed, and a faster speed of $\sim$1000 km s$^{-1}$, which is near the Alfvén speed (Cirtain et al., 2007). It had been pointed out much earlier (Shibata et al., 1992) that the base region of the coronal jet often has a particularly bright spot in the coronal-jet base, and that brightening is offset to one side of the base. Several general summaries and reviews of coronal jets have come out during different eras of coronal-jet studies (Shimojo and Shibata, 2000; Shibata and Magara, 2011; Raouafi et al., 2016; Hinode Review Team et al., 2019; Shen, 2021; Sterling, 2021; Schmieder, 2022).

It has been argued by Sterling et al. (2015) that most or all coronal jets result from the eruption of small-scale filaments, or *minifilaments* (being several times to orders-of-magnitude smaller than "typical" large-scale filaments, that erupt to make typical solar flares and coronal mass ejections), based on their study of 20 polar coronal hole jets, and building on several earlier studies of coronal jets (Nisticò et al., 2009; Moore et al., 2010, 2013; Hong et al., 2011; Huang et al., 2012; Shen et al., 2012; Adams et al., 2014). Sterling et al. (2015) proposed that the minifilament eruption and resulting coronal jet are scaled-down versions of typical filament eruptions that produce solar flares and coronal mass ejections (CMEs).

Figure 1 shows an example of a coronal jet, occurring in the south polar coronal hole. Panel 1 (a) shows the coronal jet when it is well developed, in a SXR image from the *Hinode* spacecraft. The blue arrow points to the spire, and the green arrow points to the base brightening. We call the latter a JBP for the "jet bright point" in the coronal-jet's base (this terminology is from Sterling et al., 2015). Panels 1 (b)—1 (d) show the same location in EUV images from the *SDO*/AIA instrument's 193 Å channel. Panel 1(b) shows the situation prior to the start of the coronal jet. Panel 1 (c) is from about the same time as the SXR image in 1 (a). It shows the spire less prominently than in SXRs at that moment, but it also shows a minifilament (in absorption) in the process of erupting outward (yellow arrow). These erupting minifilaments usually are, at best, only hinted at in SXR images, but are often clearly visible in at least one and often in several AIA EUV channels (Sterling et al., 2022). In 1 (d), this minifilament has continued to erupt, with portions of it leaking out into the bright spire.

Figure 2 shows the scenario proposed by Sterling et al. (2015) to explain coronal jets. This shows a coronal-hole region: most of the photospheric magnetic flux has the same polarity (negative in this case), and the ambient coronal field is open. While this drawing is tailored for a coronal hole region, the same description holds where the ambient coronal field is a long loop (compared to the size of the base region) instead, which would be common in quiet Sun and active regions. A positive-polarity patch is present in the region, and this forms an anemone-type structure (Shibata et al., 2007), with flux emanating out

of the positive patch and closing down in negative flux surrounding the positive patch in 3-D, where Figure 2(a) shows a 2-D cross-section of this structure. One lobe of the anemone - the smaller lobe on the right-hand side (i.e., the closed-field region between B and C in Fig. 2) in this depiction - contains non-potential (sheared and twisted) field, and holds a minifilament. The adjacent lobe on the left side is larger and contains more-nearly potential field. Figure 2(b) shows the minifiament, and its enveloping flux-rope field, erupting. This results in two magnetic reconnections. One reconnection occurs where the erupting-minifilament's field encounters the ambient coronal field above the larger lobe. This adds new, heated loops to the large lobe, and creates new open field, along which heated material can flow out and create the coronal-jet spire. The second reconnection occurs among the leg field of the erupting flux-rope-enveloping field. This causes a miniature flare to occur, in a fashion analogous to how typical solar flares are formed (e.g., Hirayama, 1974; Shibata et al., 1995; Moore et al., 2001). This miniature flare is what appears as the aforementioned JBP. In Figure 2(c), the erupting field has reconnected far enough into the open-field region for the cool minifilament material in the flux-rope core of the erupting field to leak out onto the open field, where it flows away as part of the spire.

Studies of coronal jets occurring on the solar disk have provided insight into the magnetic origins of the coronal-jet-producing minifilament eruptions. Panesar et al. (2016b) found that magnetic cancelation occurred at the coronal-jet location before and during the coronal jet in 10 quiet Sun jets, and in a similar study Panesar et al. (2018a) found magnetic cancelation occurring near the start of 13 coronal hole jets. Additional multiple-coronal-jet studies support these findings, including McGlasson et al. (2019) and Muglach (2021). A study of (Kumar et al., 2019) argues that "shearing and/or rotational photospheric motions" are more important than cancelation in producing coronal-hole jets that they studied; they do find, however, evidence that minifilament eruptions produce about two-thirds of the coronal jets, and that small-scale eruptions without cool-minfilament material cause the remaining ones. Magnetic cancelation has also been found to accompany many active region jets (Sterling et al. 2016, Sterling et al. 2017; Mulay et al. 2016 state that cancelation, flux emergence, or cancelation-plus-emergence produce coronal jets they observe). Single-event studies have also found cancelation to accompany coronal jets in many cases. There are several other observational examples of magnetic flux cancelation leading to minifilament eruptions that produce coronal jets (e.g., Solanki et al., 2019; Yang et al., 2019; Mazumder, 2019). See the above-mentioned reviews for additional citations.

Observations support that flux cancelation at the neutral line labeled "B" in Figure 2(a) often triggers the minifilament to erupt. Similarly, magnetic flux cancelation also likely often builds the minifilament prior to eruption, in some cases hours to ∼two days prior to its eruption (Panesar et al., 2017). If the minifilament has twist on it, perhaps supplied when canceling magnetic elements themselves contain shear derived from photospheric motions, that twist can be supplied to the coronal-jet's spire upon eruption of that minifilament and its reconnection with the coronal field, explaining why many coronal-jet spires display a spinning motion during their evolution (e.g. Moore et al., 2015).

## 2 SOME CORONAL-JET-OBSERVING INSTRUMENTS

We briefly introduce instruments often used for coronal-jet studies over recent decades. Here we describe those instruments that are referred to most in this paper. See the reviews listed in §1 for discussions of other instruments used in coronal jet observations.

In SXRs, coronal jets were first extensively observed with the *Yohkoh*/Soft X-ray Telescope (SXT; Tsuneta et al., 1991), which operated from 1991—2001. It had a detector with square pixels of width

$2\farcs455$, and variable cadence with the fastest being about 2 seconds, although it often ran with much coarser cadence. Its followup was the X-ray Telescope (XRT; Golub et al., 2007) on the *Hinode* satellite, launched in 2006, and still operating as of this writing. It has pixels of width $1\farcs02$, and — for observations most appropriate for coronal jets — operated with a cadence of $\sim$30 seconds. Both SXT and XRT imaged with variable field of view (FOV), although for cadences sufficient to observe coronal jets of $\sim$10-minute lifetime both instruments used a FOV smaller than that of the full solar disk.

With *Yohkoh*/SXT, a large percentage of observed coronal jets occurred in active regions, with very few seen in polar regions (Shimojo et al., 1996). Koutchmy et al. (1997) did see some polar coronal hole jets with SXT, but only with relatively long exposures of 15 and 30 seconds. In contrast, coronal jets are very prominent and common in polar regions in *Hinode*/XRT observations (Cirtain et al., 2007). As discussed in Hinode Review Team et al. (2019) (in the subsection on coronal jets), this difference in visibility between the two SXR-imaging instruments can be understood because the filters that see the coolest SXR plasma with *Yohkoh*/SXT had sensitivity that dropped off sharply below about 2 MK, while the coolest filters of *Hinode*/XRT have good sensitivity to plasmas of down to just under 1 MK. From filter-ratio temperature studies, Nisticò et al. (2011), Pucci et al. (2013), and Paraschiv et al. (2015) determined that polar-coronal-jet spires have temperatures of $\sim$1—2 MK. Therefore this could explain why they are easily visible in images from the cooler-temperature-detecting *Hinode*/XRT, but much-less visible or invisible in images from the hotter-temperature-detecting *Yohkoh*/SXT.

For EUV observations, although there were some earlier useful observations with the EUV Imager (EUVI) telescope on the *STEREO* spacecraft (Nisticò et al., 2009, 2010), the results discussed in the present paper largely derive from the Atmospheric Imaging Assembly (AIA; Lemen et al., 2012) on the Solar Dynamics Observatory (*SDO*) satellite, which has been operational from 2010, and is still operational as of this writing. It has a detector of $0\farcs6$ pixels, and regularly observes the entire solar disk with 12 second cadence in seven EUV channels centered at 304, 171, 193, 211, 131, 335, 94 Å, roughly in order from detectability of the coolest to the hottest plasmas for non-flaring situations (the details of the ordering depend on the distribution of temperatures in the emitting plasmas, and also some channels have good response in multiple temperature ranges; Lemen et al. 2012 gives the AIA response curves and principle ions contributing to each wavelength band). Sterling et al. (2015) found that polar coronal hole jets are best visible in the first four of these channels, and that the hotter channels of 131, 335, and 94 Å added little new information. Active region jets, which tend to be hotter than the polar coronal hole jets, generally are well seen over a broader range of AIA channels. Shimojo and Shibata (2000) found active region jets to have temperatures 3—8 MK, based on SXT filter-ratio methods, and later studies have also found active region jet temperatures in this range (Paraschiv et al., 2022).

Several papers by Mulay et al. (2016, 2017b,a) use the EUV Imaging Spectrometer (EIS) on *Hinode* to undertake spectroscopic studies of coronal jets, and survey a broader temperature range than that of the SXR filter-ratio methods of the just-mentioned studies. They report the bulk of the emission of active-region-jet spires to be of temperatures $\lesssim$1—2 MK. This is substantially lower than the active-region-jet temperatures from the filter ratios mentioned above, e.g., the 3—8 MK of Shimojo and Shibata (2000). But this difference is likely due to the nature of the plasmas that the respective instruments can detect. EIS, being an EUV spectrometer, has spectral coverage of substantially cooler spectral lines than those contributing to the SXR emission. Thus it is likely that there is a wide distribution of plasma temperatures in coronal jets, and – not surprisingly – the SXR telescopes preferentially detect the hotter plasmas in those coronal jet spires, and therefore yield higher temperatures for coronal jets than the bulk of the coronal-jet plasmas detected by EIS.

Spectroscopy in the UV from *IRIS* has provided valuable insight into coronal jets. This includes studies finding rotational (spinning) motion in coronal jets (e.g., Cheung et al., 2015; Liu et al., 2018; Schmieder et al., 2022; Ruan et al., 2019), confirming indications of such rotation from earlier observations in EUV (Pike and Mason, 1998). These spectra also provide information on densities in coronal jets (e.g., Cheung et al., 2015; Mulay et al., 2017b; Panesar et al., 2022). Moreover, the high resolution of the *IRIS* slitjaw images can complement the EUV and SXR coronal-jet observations in, for example, zeroing in on the fine-scale structure and dynamics at the coronal-jet magnetic-source location in the photosphere (Sterling et al., 2017).

Magnetograms from the *SDO* Helioseismic and Magnetic Imager (HMI; Scherrer et al., 2012) is frequently used to study the photospheric magnetic flux values and changes around the base of coronal jets. HMI has pixels of $0\farcs5$, and takes a line-of-sight magnetogram of the full solar disk once every 45 seconds.

## 3 CORONAL JETS AND JET-LIKE ACTIVITY ON DIFFERENT SIZE SCALES

### 3.1 Coronal-jet Physics on Large Scales

Coronal jets appear to be small-scale versions of larger eruptions, with the eruptive process that results in a minifilament eruption that produces a coronal-jet spire and a JBP corresponding to large-scale eruptions that result in filament eruptions and typical solar flares (Sterling et al., 2015). That is, just as "typical" solar filaments erupt (in what we are here calling "large-scale eruptions") to make long-observed "typical" solar flares and that sometimes expel coronal mass ejections into the heliosphere, coronal-jets appear to be made by a minifilament eruption (a scaled-down version of a large-scale filament eruption) that leaves in its wake a JBP (a scaled-down version of a typical solar flare), and to result in material and magnetic disturbances that flow out along a spire and that sometimes flow into the heliosphere.

If coronal jets are indeed a scaled-down version of larger "standard flare model" solar eruptions, then we would expect other aspects of the smaller-scale eruptions that cause coronal jets and JBPs to have counterparts in the larger-scale eruptions that cause CMEs. Here we discuss examining large-scale eruptions based on what has been found in coronal jets.

A characteristic of coronal jets is the anemone magnetic setup, similar to that shown in Figure 2(a). There are many examples of flares occurring from anemone active regions (Asai et al., 2009; Lugaz et al., 2011; Kumar and Manoharan, 2013; Devi et al., 2020). Joshi et al. (2017) showed that the setup for a large-scale eruption matched that of the coronal-jet minifilament-eruption picture, and that the dynamic motions of the eruption matched closely that of an erupting minifilament producing a coronal jet. A similar schematic was in fact drawn to explain a series of recurring solar eruptions much earlier (Sterling and Moore 2001, 2001, 2001; these schematics in fact helped inspire the Fig. 2 schematic of Sterling et al. 2015). These setups show that the same type of magnetic setup appears to be capable of generating similar solar expulsions both on the coronal-jet size scale, and on the size scale of typical solar eruptions. Whether a coronal jet results or a CME results depends on how much of erupting minifilament/flux-rope lobe remains after the external reconnection in Figure 2(b) and 2(c). If the flux rope is robust enough to survive that reconnection (that is, if only the outer portion of the flux-rope lobe is eroded away by external reconnection), then the remaining lobe and flux rope can escape to form a CME that carries a magnetic flux rope in its core region. If on the other hand the external reconnection totally reconnects the flux rope, so that the field lines that were previously closed in a flux rope all become open, then the feature becomes a coronal jet instead of a CME.

An anemone setup appears to be necessary for coronal-jet formation, and formation of coronal jets in such a setup is supported by numerical simulations (Wyper et al., 2017, 2018a,b; Wyper et al., 2019; Doyle et al., 2019). But large-scale eruptions also occur outside of an anemone setup, and so we might ask whether the eruptions of minifilaments that cause coronal jets might also have similarities to larger-scale eruptions, independent of whether those larger-scale eruptions occur in an anemone configuration. One possible such similarity is in the manner in which the minifilament eruptions and the large-scale eruptions are triggered to erupt. We have seen above that coronal-jet-producing erupting minifilaments are apparently often built-up and triggered to erupt by magnetic-flux cancelation. What about larger-scale eruptions?

To investigate whether large-scale eruptions are built up and triggered to erupt in a manner similar to coronal-jet-producing minifilament eruptions, Sterling et al. (2018) studied how large-scale eruptions evolve toward eruption. In the case of coronal jets, the magnetic elements taking part in the cancelation typically converge toward each other over the hours prior to the eruption onset, as discussed in several papers (Panesar et al., 2016b, 2017, 2018a; Sterling et al., 2017), and as exemplified by Figure 3(c). This time period is short enough for those elements to have relatively little interaction with surrounding flux elements. In contrast, large-scale eruptions often occur in active regions that develop for many days, or even weeks, prior to expelling an eruption (complex regions, such as delta regions, can evolve faster than this, but the objective of Sterling et al. 2018 was to compare with more standard eruptions). Thus, in order to follow the region from the time of flux emergence through to the time of the eruption, it was necessary to look at regions that were small enough for this evolution to occur during a single disk passage of the region. Sterling et al. (2018) presented two examples of this class. In both cases the active regions were comparatively small bipolar active regions (total flux in each $\lesssim 10^{21}$ Mx). Also in both cases the eruptions occurred about five days after emergence, and those eruptions produced CMEs observed in coronagraphs. One of the regions remained almost completely isolated from any surrounding substantial flux over this period. And the second (shown in Fig. 4) was largely isolated from surrounding flux, although one of its polarities did have some interaction with nearby pre-exisiting opposite-polarity flux.

Both regions displayed similar evolution. Figure 4 shows the evolution of one of these regions. The boxed region in (a) shows a bipolar active region that is still emerging in this frame. In panel (b) the emergence is continuing, with centroids of the the main positive-polarity (white) and negative-polarity (black) patches further separated from their central neutral line than they were in (a). By the time of (c) however, they are no longer separating, and some of the opposite-polarity portions of the region have converged toward the central neutral line. Panel (d) shows a time-distance map of this region, analogous to that in Figure 3(c). This shows that the polarities initially separate for about one day following their initial emergence. Their mutual directions then reverse, and the polarities start to converge. The orange line shows on this plot the time of the CME-producing eruption; this did not occur until after the polarities had converged on each other, and were undergoing flux cancelation along their central neutral line. There were no CME-producing eruptions from this region prior to this time. *SDO*/AIA observations show that the bright centroid of the resulting *GOES* C-class flare was on that neutral line. Thus, similar to the situation with coronal jets, a flux rope eruption occurs along a cancelation neutral line. In this case, the region evolved for about four days with essentially no activity, and then had an eruption only after that cancelation started taking place.

A second region examined in Sterling et al. (2018), which also was substantially isolated magnetically from surrounding structures, began with flux emergence, underwent flux-polarity separation, and then had flux convergence and apparent cancelation along its central neutral line among some portion of its two opposite-polarity patches. This resulted in a eruption that produced a *GOES* B-class flare on the region's central neutral line (although in this case a second, weaker, eruption also occurred on a neutral line formed

from one of the emerging polarities and a pre-existing opposite polarity patch), and in the expulsion of a CME.

Chintzoglou et al. (2019), studying more complex magnetic situations involving multiple active regions, also found that eruptions occurred at flux-cancelation neutral lines.

Returning to the discussion of the size scale of the erupting minifilaments that can cause coronal jets, Moore et al. (2022) examined the evolution of 10 bipolar ephemeral active regions (BEARs) in a manner similar to Sterling et al. (2018), but where they tracked their regions from emergence to disappearance. These 10 regions produced 43 small-scale eruptions in total, and all of these eruptions occurred at a neutral line in which apparent flux cancelation was taking place. This again supports that the the physics that causes eruptions on the coronal-jet size scale is essentially the same as that which causes large-scale eruptions that produce typical solar flares and CMEs.

These observations strongly support that flux cancelation is often essential in the magnetic build-up and triggering of both smaller-scale eruptions that cause coronal jets, and larger-scale eruptions that cause flares and CMEs. This is fully consistent with the mechanism for the build-up of the non-potential energy required for eruption via flux cancelation, as suggested by van Ballegooijen and Martens (1989). Observations of these processes occurring on faster time scales in the smaller-size-scale jets, however, helps to elucidate strategies for investigating the processes in the more-slowly developing larger active regions.

### 3.2 Possible Extensions to Smaller Scales

From the preceding discussions, we have presented evidence that the same basic process leading to eruptions occurs on two size scales – that of large-scale eruptions and that of coronal jets. Sterling and Moore (2016) considered a possible extended relationship to smaller size scales, by plotting the the size of a typical filament or filament-like structure that erupts on one axis, and, on the other axis, a measure of the number of the respective eruptive events occurring at any given time on the Sun. Their motivation was to see whether a substantial number of similar features might occur on a spicule size scale, assuming that the coronal-jet mechanism continues to scale downward to sufficiently small sizes. If so, then it might be that at least some spicules (and perhaps many or most spicules) result from erupting filament-like features (erupting flux ropes) of that size scale. (See §3.4 for a summary of spicule properties.)

The larger of the two size scales of eruptive events that have observed filament eruptions are the "typical" filament eruptions that have solar flares occurring beneath them, and – in the case of ejective eruptions – expulsion of a CME. Sterling and Moore (2016) took a typical eruptive filament size to be 70,000 km, with an appropriate scatter based on observed values for a large number of filaments by Bernasconi et al. (2005). For the number of large-scale eruptions, they took observed CME rates of from less than one to a few per day (Yashiro et al., 2004; Chen, 2011). For coronal jets, they estimated corresponding numbers for the size of erupting minifilaments based on measurements in Sterling et al. (2015), which on average was just over 5000 km for the erupting-minifilament lengths. For the frequency of eruptions they extrapolated rates given in Savcheva et al. (2007), which yields about a few hundred per day over the entire Sun.

In order to compare with spicule occurrence rates, Sterling and Moore (2016) converted the occurrence rates for the large-scale eruptions and coronal-jet-size-scale minifilament eruptions to the expected number of events occurring on the Sun at any random given time. The motivation for these units was to utilize the historical studies of spicule counts, which were sometimes expressed as the total number of spicules on the Sun seen at a given time. Those resulting values vary substantially (Athay, 1959; Lynch et al., 1973),

but overall they are roughly in the neighborhood of $10^6$ spicules on the Sun at a given time. (Judge and Carlsson 2010 estimate about a factor of ten higher; see Sterling et al. 2020a.)

In order to complete the comparison with the larger erupting features, a value for the typical size of the erupting filament-like flux rope that would produce a spicule is required. No such cool-material eruptions have been convincingly observed to date, and therefore spicules being formed by the coronal-jet-producing minifilament-eruption-type mechanism is wholly speculative at this point. But because coronal-jet-spire widths are similar to the measured lengths of the erupting minifilaments that produce them, by analogy, Sterling and Moore (2016) hypothesized that there might be erupting *micro*filaments (erupting micro flux ropes) of lengths comparable to the width of spicules (a few hundred km), that produces some spicules.

Figure 5 shows the resulting plot. When a linear extension is made from the large-scale eruptions through the coronal-jet-sized eruptions, and then extended down to the size scale of the putative erupting microfilaments, the ordinate's value for their occurrence rate falls near the lower end of the estimated spicule-number counts. This implies that at least some portion of spicules might be scaled-down versions of coronal jets, formed by eruptions of microfilaments, or it could be that multiple spicules are produced by a single such eruption.

We next consider from an observational standpoint the suggestion that the coronal-jet-producing mechanism operates on size scales smaller than that of coronal jets.

### 3.3 Jetlets

Raouafi and Stenborg (2014) studied long and narrow transient features of a scale smaller than coronal jets, using *SDO*/AIA images and HMI magentograms. They called these features *jetlets*, due to their similarity to coronal jets, except having a smaller size (both width and length). Jetlets are smaller than coronal jets, but larger than chromospheric spicules. Raouafi and Stenborg (2014) found the jetlets to occur at the base of coronal plumes, and they suggest that they (along with transient base brightenings) are the result of "quasi-random cancellations of fragmented and diffuse minority magnetic polarity." Therefore, these features seem to be smaller versions of coronal jets. ("Plumes" are long and narrow features – first noticed during total eclipses – extending out to several solar radii in polar regions. Compared to jet-like features, plumes are long-lasting, persisting for $\sim$day. See, e.g., Poletto 2015.)

Panesar et al. (2018b) examined jetlets with *IRIS* UV and AIA EUV images, and HMI magnetograms. They studied ten jetlets, and found them to have lengths $\sim$27,000 km, spire widths $\sim$3000 km, base size of $\sim$4000 km and speed $\sim$70 km s$^{-1}$. They argued that jetlets are a more general solar feature than presented in Raouafi and Stenborg (2014), occurring at the edges of chromospheric network both inside and outside of plumes. In agreement with Raouafi and Stenborg (2014), they found that magnetic flux cancelation was the likely cause of the jetlets, just as it often leads to coronal jets. Furthermore, their jetlets were accompanied by brightenings analogous to the JBP seen at the base of coronal jets. Based on these and other characteristics, Panesar et al. (2018b) concluded that the jetlets are likely scaled-down version of coronal jets, and that they are consistent with the erupting-minifilament scenario for their production. They did not, however, observe a clear indication of the existence of an actual cool-material erupting minifilament at the base of their jetlets.

Panesar et al. (2019) extended these studies to even smaller-sized jetlets, using EUV 172 Å (Fe IX/Fe X) images from the Hi-C 2.1 rocket flight. This instrument had pixels of width $0\farcs129$, and cadence of 4.4 seconds; see Rachmeler et al. (2019) for details. Six events were identified from the data from Hi-C 2.1's five-minute flight. As with the Panesar et al. (2018b) jetlet study, these events also occurred at the

edges of network cells. On average they had spire lengths of ∼9000 km, widths of 600 km, and speeds of ∼60 km $s^{-1}$. At least four of these events seemed consistent with being small-scale coronal jets following the erupting-minifilament mechanism, although once again there were no direct observations of erupting cool-material minifilaments.

### 3.4 Spicule-sized Features

Spicules are chromospheric features that are extremely common, have lengths ∼5000—10,000 km, widths of a few hundred km, lifetimes of a few minutes, and cluster around the magnetic network (e.g. Beckers, 1968, 1972). Although many ideas exist, their generation mechanism is still unknown; see discussions in various review works (e.g., Beckers, 1968, 1972; Sterling, 2000; Tsiropoula et al., 2012; Hinode Review Team et al., 2019; Sterling, 2021).

As mentioned in §3.2, erupting microfilament flux ropes have not been observed in spicules. They may, however, be present, but hard to observe for a variety of reasons. Similarly, a bright point that corresponds to a JBP has not been convincingly observed at the base of spicules. These points are not consistent with an erupting-microfilament mechanism for spicules. Nonetheless, these absences are not definitive evidence that these features do not exist in spicules; they may exist but be hard to detect, as discussed in Sterling et al. (2020a).

Moreover, there are several observations that are consistent with a microfilament-eruption mechanism for spicules. One of these is the observation of mixed polarity elements at the base of many spicules. Fresh evidence for this is presented in Samanta et al. (2019), obtained using state-of-the-art ground-based observations in the pre-DIKIST era. This work presents evidence that spicules result from dynamic activity at the base of spicules, which could be due to flux cancelation and/or emergence. As discussed above, there is extensive evidence that many coronal jets result from flux-cancelation episodes. Ideas for coronal-jet production from flux emergence has also been presented (Yokoyama and Shibata, 1995).

Spicules also display characteristics of spinning motions (Pasachoff et al., 1968; De Pontieu et al., 2012; Sterling et al., 2020b). We have noted that the minifilament-eruption idea offers an explanation for the spinning of coronal jets, when an erupting twisted minifilament transfers its twist to the coronal-jet-spire's coronal field via external reconnection. Thus the same mechanism acting on speculative erupting microfilaments might explain this spicule spinning as magnetic untwisting.

There remains, however, the possibility that spicules are driven by any of a number of other suggested mechanisms (see the above-cited reviews), and many of these ideas cannot yet be ruled out. Spicule-sized features that work via the coronal-jet-production mechanism may instead drive other features of that size, such as the UV network jets described by Tian et al. (2014) (some of which are UV observable in EUV, at least in AIA 171 Å images; Tian et al., 2014), or the "chromospheric anemone jets" observed in active regions, or similar jet-like features observed in plages (De Pontieu et al., 2004; Sterling et al., 2020a).

## 4 THE IMPORTANCE OF CORONAL JETS

Coronal jets are important for solar physics in a number of ways. One of these is to gain insight into the buildup and onset of large-scale eruptions. Studies of these eruptions has importance in a variety of areas, ranging from the understanding of key inputs to Space Weather to gaining insight into fundamental astrophysical processes.

One of the key unknowns of solar physics is the details of the mechanism leading up to and causing large-scale solar eruptions that produce typical-sized-filament eruptions, solar flares, and CMEs. The revelation that many coronal jets are scaled-down versions of large eruptions has important implications for resolving these questions. Not only are coronal jets of a smaller size scale than those large eruptions, but also the pre-coronal-jet evolution time scale of coronal jets is substantially shorter than that for large eruptions: Large eruptions from bipolar active regions usually require at least many days to build up the magnetic circumstances that result in the eruption (e.g., Sterling et al., 2018), while in contrast, for a sample of quiet-region jets the corresponding time scale was found to be of the order of hours or a couple of days (Panesar et al., 2017). Additionally, it is difficult to find examples of magnetically isolated large-scale regions that produce large eruptions for many days while they remain on the Earth-facing side of the Sun, and this exacerbates the difficulty in unraveling the fundamental processes that lead to eruptions. On the other hand, it is often easy to find and follow coronal-jet-producing regions on the Sun, by working backwards from the time of coronal-jet occurrence. As discussed in §3.1, Sterling et al. (2018) used these points to learn about regions leading to flares and CMEs in two small active regions, largely based on lessons learned from coronal-jet studies. These studies and comparisons are, however, still vastly incomplete. Careful study of the details of eruptions happening on the coronal-jet-sized scale are necessary to understand fully the coronal-jet-production process. And then the findings can be used as starting input for improved studies of large-scale events.

And as demonstrated in §3.2, coronal jets almost certainly can provide insight into the operation of some smaller-scale events. This is in particular true for those smaller objects with the most apparent coronal-jet-like qualities; this includes jetlets, at least some of which must be scaled-down versions of coronal jets. It will be important to see how far the obvious similarities continue down in size scale by using long-term high-resolution and high-cadence observations at appropriate wavelengths. This will help determine whether the similarities continue down to the size of the UV network jets, which are nearing spicule size. Because the solar wind appears to originate from most if not all locations on the Sun (in particular, the fast solar wind originates from open-field areas, while the slow wind comes from closed-field regions), the solar-surface events that drive it are likely distributed almost uniformly over the surface. An understanding of jetlets and UV network jets will provide insight into whether these events plausibly power the solar wind. Careful additional coronal-jet studies are required to guide and assist observational investigations of these yet smaller-scale features.

Coronal-jet physics may have even broader implications beyond the most obvious looking coronal-jet-like or solar-eruption counterparts. For example, Katsukawa et al. (2007) have examined "penumbral jets," rooted along the filament-like low-lying magnetic loops (the penumbral fibrils) that spread radially from sunspot umbra and form the penumbra (Tiwari et al., 2013). Tiwari et al. (2016, 2018) also studied penumbral jets, and found that large ones originated from the end of the penumbral filament rooted farthest away from the umbra, and that these regions had mixed magnetic polarities that underwent magnetic cancelation near the time of penumbral-jet generation. Moreover, using *IRIS* spectra, they found Doppler evidence that the penumbral jets are undergoing spinning motion. Although these penumbral jets are $\sim$100 times smaller than typical SXR coronal jets, their properties of magnetic cancelation at their bases, long (compared to their width) spires, and spin, are similar to what has been found in numerous coronal jets. This suggests that the basic physical mechanism creating these penumbral jets might be essentially the same as that which produces coronal jets.

"Campfires" are features recently discovered in high-resolution EUV images from the Extreme Ultraviolet Imager (EUI) on the *Solar Orbiter* spacecraft, appearing as small localized brighteings of size scales of a

few 100—few 1000 km and lasting 10—200 seconds (Berghmans et al., 2021). By comparing a selection of campfires with *SDO*/HMI magentograms, Panesar et al. (2021) present evidence that they occur on canceling magnetic neutral lines, similar to how coronal-jet-producing erupting minifilaments and accompanying base brightenings also frequently occur on canceling neutral lines. This suggests that the same process that makes coronal jets (small-scale-filament/flux rope eruptions) might also make campfires.

If the same processes indeed make features as varied as large-scale solar eruptions, coronal jets, jetlets, some spicules, UV network jets, campfires, penumbral jets, and perhaps other features, then it is important for heliophysics to clarify which magnetic and physical circumstances produce which feature in what situations.

Coronal jets also have influence far out into the heliosphere. White-light coronagraph images show that some CMEs are relatively narrow, with angular extents $\lesssim 5^\circ$; these features have been called both "narrow CMEs" and "white-light jets" (See discussion and references in Sterling, 2018). Wang et al. (1998) have shown that these features often originate from jetting activity at the solar surface, and a mechanism for producing these features has been presented, based on the minifilament-eruption picture, by Panesar et al. (2016a). Sterling and Moore (2020) present observations of material expelled from coronal jets extending out to tens of solar radii in images from the *STEREO* "Hi1" Heliospheric Imager. There is also evidence of *in situ* detection of coronal-jet material in the solar wind (Yu et al., 2014, 2016). Both (Sterling and Moore, 2020), and a followup work (Neugebauer and Sterling, 2021), suggest that coronal jets, and/or smaller jet-like features that work via the minifilament-eruption mechanism, might propagate out to the heliospheric locations of the *Parker Solar Probe* satellite, and be detected as magnetic Alfvénic kinks in the field that are known as "switchbacks" (Bale et al., 2019; Schwadron and McComas, 2021). The idea is that the erupting minifilaments might carry twist, and external reconnection with the ambient coronal field could transfer that twist to the field, as described by Shibata and Uchida (1986). That twist could convert to swaying of inner coronal field (Moore et al., 2015), and then steepen into an Alfvénic kink – forming the switchback – due to variations of the Alfvén speed in the solar wind (Sterling and Moore, 2020). Switchbacks are extremely common in the solar wind at distances of a few tens of solar radii (Bale et al., 2019). They also appear to carry the imprint of size scales at the Sun corresponding to supergranules (Bale et al., 2021; Fargette et al., 2021), and even of granules (Fargette et al., 2021). The minifilaments that erupts to make coronal jets ($\sim$10,000—few $\times$10,000 km; e.g., Sterling et al., 2015; Panesar et al., 2016b) are not so different from supergranule scales ($\sim$40,000 km), while the width of spicules and similar features (few 100 km or so) is not too different from the size scale of granules ($\sim$1000 km). Better observations of coronal jets can help determine whether this switchback-production idea matches detailed observations, or whether a different mechanism might be responsible for the switchbacks, such as "interchange reconnection" ideas (e.g., Zank et al., 2020; Owens et al., 2020; Drake et al., 2021; Schwadron and McComas, 2021), or any of several ideas for generating the switchbacks in the solar wind (see citations in Fargette et al., 2022), while keeping in mind that the mechanism should explain the observations of a supergranule- and/or granule-size-scale dependence of switchback size scales.

These points illustrate the value to solar physics – and beyond – of understanding the nature of the processes that lead up to and produce coronal jets. To this end, we suggest a new instrument focused on observing coronal-jet-sized features in the low corona. We first note, however, that another reason for further observations of coronal jets is to learn more about the nature of coronal jets themselves. Even though there is strong evidence that the minifilament eruption model explains many coronal jets, it is still to be confirmed that the model holds up to close scrutiny under improved observations. An alternative mechanism, which was originally proposed along with the earliest detailed coronal-jet observations (Shibata

et al., 1992), is that they result when emerging magnetic flux reconnects (external reconnection) with surrounding coronal field. As mentioned in §1, many observations fit the minifilament-eruption model and find that coronal jets frequently occur as the result of minifilament (or flux rope) eruptions on canceling magnetic neutral lines. Other observations of coronal jets – such as the direction of motion of coronal-jet spires horizontal to the solar surface – are also consistent wtih the minifilament-eruption mechanism and not with the emerging-flux mechanism (Baikie et al., 2022). So questions are: do coronal jets ever form via the emerging-flux mechanism, and if so, are there any special characteristics of those coronal jets compared to those that we have described in §1? Another question is, if coronal jets do not occur frequently via the emerging-flux mechanism, then why not? After all, numerical simulations indicate that flux emerging into open surrounding coronal field should produce a coronal jet (e.g., Yokoyama and Shibata, 1995; Nishizuka et al., 2008). So if that process does not produce coronal jets on the Sun in reality, then it is important to understand why the reconnection resulting from flux emergence (which inevitably must happen) does not produce actual coronal jets. These questions emphasize the importance of understanding physics on the size scale of coronal jets.

## 5 THE "SEIM" INSTRUMENT TO OBSERVE CORONAL JETS AND JET-LIKE STRUCTURES

We propose a new instrument for the next generation, under the provisional name of the "Solar Explosions IMager" (SEIM). This instrument would be tuned to observe features of size scales of coronal jets at EUV wavelengths, with a spatial resolution and cadence similar to that of the Hi-C2.1 instrument. The Hi-C flights, however, were on sounding rockets, and so of short duration ($\sim$5 min). The *Solar Orbiter*/EUI instrument can also achieve high resolution comparable to that of Hi-C, but such high resolution is only available for a few days around *Solar Orbiter*'s perihelion. Our idea is for SEIM to be on a satellite, allowing for long-term high-resolution observations. We now outline the instrument's desired characteristics.

### 5.1 Wavelength Coverage

As pointed out in §2, coronal jets in polar coronal holes such that the spires are generally seen in the *SDO*/AIA channels of 304, 171, 193, and/or 211 Å. Among these, 171, 193, and 211 are all coronal lines. It would be best to include all of these channels, as sometimes the spire tends to be better seen in one than the other. Nonetheless, if it is visible in one of these three channels, it is usually at least detectable in the other two, based on observations of 41 coronal jets in Sterling et al. (2015) and Sterling et al. (2022). Therefore, as a minimum, one of these three channels should be included in a minimal mission. The 304Å channel shows a mixture of what might be called "upper"-chromospheric and transition region plasmas.. It sometimes shows features of coronal jets detected in SXRs that are not apparent in the other three cool-coronal (171, 193, 211 Å) channels (Sterling et al., 2022), and therefore that channel would be essential to include in a SEIM mission.

Brighter coronal jets, such as those occurring at the periphery of active regions, are often visible in all AIA EUV channels. Therefore, an instrument designed to see coronal-jet-like features in coronal holes (and quiet Sun) well would also be able to see coronal jets and similar features in active regions.

A channel that shows photospheric emissions, such as AIA's 1600 Å channel, would be essential to facilitate comparisons with other instruments such as DKIST. This channel also shows ribbon-like flare emission at the base of some active-region jets (Sterling et al., 2016).

Given these considerations, a minimal wavelength-coverage package for a SEIM instrument could be 304, 171 or 193, 94, and 1600 Å.

### 5.2 Resolution, Cadence, and Field of View

In active regions, some strands of erupting minifilaments are substantially thinner than the width of erupting minifilaments in coronal holes or quiet regions, having widths of $\lesssim 2''$ (Sterling et al., 2016). Hi-C, either in its original incarnation (Kobayashi et al., 2014) or the Hi-C2.1 version discussed above (§3.3), would be able to resolve many of these, and in general sees features at the limit of or beyond what is readily detectable in AIA (e.g., Brooks et al., 2013; Tiwari et al., 2016; Panesar et al., 2019; Tiwari et al., 2019; Sterling et al., 2020a). Based on this, we are confident that a resolution comparable to that of Hi-C ($0\farcs1$ pixels) will be adequate for revolutionary breakthroughs in the study of coronal jets and similar-sized phenomena.

For coronal-jet studies, the 12-second cadence of AIA has been adequate. Smaller-scale jet-like features can have lifetimes shorter than the ∼tens of minutes of coronal jets, including ∼one minute for small jetlets (Panesar et al., 2018b) and UV network jets. Therefore a faster-than-AIA time cadence comparable to that of Hi-C, about 5 seconds, would be preferred in order to sample these objects well.

A FOV of about $6' \times 6'$, would be acceptable for an initial mission. This would be slightly larger than the $4'.4 \times 4'.4$ Hi-C2.1 FOV (Rachmeler et al., 2019). *SDO*/AIA's detector is a circle of diameter $41'$ (Lemen et al., 2012), and so our proposed detector would have a FOV of about one-sixth that of AIA's. Thus we could obtain our goal of $0\farcs1$ with a FOV one-sixth that of AIA's, by using an AIA-sized detector ($4096 \times 4096$ pixels$^2$). Advances in technology might make it feasible to improve upon this, allowing for increased FOV and/or higher resolution, but these minimal criteria would allow for substantial advancements in our understanding of coronal jets and jet-like features. Figure 6 shows a sample image from XRT with a FOV similar to that being discussed (that image's FOV is only slightly larger, at $6'.67 \times 6'.67$), with much of the northern polar coronal hole and several X-ray coronal jets visible.

### 5.3 Orbit, Accompanying Instrumentation, and Operations Planning

Ideally, a mission carrying a SEIM instrument would have extended, uninterrupted views of the Sun. Accordingly, a Sun-synchronous orbit, such as that of *Hinode* (Kosugi et al., 2007) or *IRIS* (De Pontieu et al., 2014) would be appropriate, allowing for ∼nine mouths of uninterrupted viewing, and ∼three months with orbits that include spacecraft nights while still allowing ∼one hour of solar observing per orbit. Longer periods of uninterrupted viewing would be possible from L1 or a similar location, but that might be more appropriate for a more extensive followup mission.

An imaging-only mission plan would be of limited value for advancing the science of jet-like features. As a minimum, systematic corresponding line-of-sight magnetograms would be essential to complement these observations. This could be included on the same spacecraft, in which case a magnetogram FOV comparable to that of the EUV instrument would be acceptable. Alternatively, it would be possible to use synoptic full-disk magnetograms from elsewhere if appropriate ones are available; for example, it would be fully acceptable to rely on magnetograms from *SDO*/HMI or a similar instrument on a different satellite that is operational at the time of a SEIM mission. In either case, the time cadence should be about ∼1 minute, comparable to that of *SDO*/HMI (45 seconds). Spatial resolution of HMI's level would be the minimum desired, but would be adequate for an initial mission. For special programs, coordinated observations with DKIST or other ground-based instruments (such as BBSO; e.g., Samanta et al., 2019) would allow for much higher-resolution magnetograms. It will also be extremely valuable to have spectroscopic observations at

UV and/or EUV, or even SXR, wavelengths, to obtain diagnostic information on the observed objects. These spectra should have sufficient spatial and spectral resolution and high-enough cadence to address questions such as whether jetlet, UV network jet, and even spicule-sized objects routinely display characteristics of jets, such as spinning motion of their spires.

We know that coronal jets are common in polar coronal holes, and they are observed in on-disk coronal holes also. Therefore, a basic minimal-maintenance plan would be to observe (with tracking) an on-disk coronal hole when one is available. This would allow for coordination with line-of-sight magentograms. A second low-latitude target would be active regions. The frequency of typical coronal jets from active regions is not yet known, but they are not uncommon. Even in the absence of such coronal jets, there are smaller-scale penumbral jets that that are ubiquitous in active regions, and it would be desirable to have high-resolution, high-cadence observations of other active-region activity, and of course it would be highly desirable for the instrument to observe large-scale eruptions from active regions. In the absence of on-disk coronal holes and active regions (or if there are only active regions showing essentially no substantial activity), one of the two polar regions (preferably one with a prominent coronal hole) would be the standard default target.

### 5.4 Extensions

The instrument proposed here could act as a proving ground for a more elaborate mission that features a full-disk FOV and wider wavelength coverage. This would be analogous to how the *TRACE* mission (Handy et al., 1999) preceded AIA on *SDO*. It would be fully appropriate for such a more-extensive mission to operate from L1 or similar location, with uninterrupted solar viewing. Such an instrument would ideally be accompanied by a complementary magnetograph, and perhaps other instruments, on the same spacecraft.

The Appendix provides a summary of properties of coronal jets and jet-like features that will be either observed directly with SEIM, or to which SEIM will provide valuable supplementary observations, for refining our understanding of all of these features.

Even in the simplest form however, the SEIM instrument suggested above would be far more than just a "solar-jets telescope." As we have argued above, solar jets can be viewed as a proxy for one of the many types of possibly similar solar features, on both larger and smaller size scales, that could be observed and studied in detail with such as instrument. Therefore, SEIM would provide a new, high-resolution, high-time-cadence window into an understanding of fundamental explosive phenomena that occur on multiple size scales in the lower solar atmosphere, and that possibly power the heliosphere as well.

## CONFLICT OF INTEREST STATEMENT

The authors declare that the research was conducted in the absence of any commercial or financial relationships that could be construed as a potential conflict of interest.

## AUTHOR CONTRIBUTIONS

ACS collected all materials and authored the bulk of the manuscript. RLM consulted on all aspects of the content. NKP contributed consultations and input into coronal jet and jetlet details. TS contributed consultations and input into spicule observation and analysis details. SKT contributed consultations and input into sunspot and penumbral jet details. SS critiqued the manuscript and provided valuable feedback.

## ACKNOWLEDGMENTS AND FUNDING

This paper expands upon material presented previously in a white paper submitted to the National Academies of Sciences, Engineering, and Medicine for the U.S. Solar and Space Physics (Heliophysics) Decadal Survey, for Heliophysics 2050 (Sterling and Moore, in press 2022).

ACS, RLM, and NKP were supported with funding from the Heliophysics Division of NASA's Science Mission Directorate through the Heliophysics Supporting Research (HSR, grant No. 20-HSR20_2-0124) Program, and the Heliophysics Guest Investigators program. ACS and RLM were supported through the Heliophysics System Observatory Connect (HSOC, grant No. 80NSSC20K1285) Program. ACS received additional support through the MSFC *Hinode* Project, and NKP received additional support through a NASA SDO/AIA grant. SKT gratefully acknowledges support by NASA HGI (80NSSC21K0520) and HSR (80NSSC23K0093) grants, and NASA contract NNM07AA01C (*Hinode*). *Hinode* is a Japanese mission developed and launched by ISAS/JAXA, with NAOJ as domestic partner and NASA and UKSA as international partners. It is operated by these agencies in co-operation with ESA and NSC (Norway). We acknowledge the use of data from AIA and HMI data, both of which are instruments onboard *SDO*, a mission of NASA's Living With a Star program.

## DATA AVAILABILITY STATEMENT

No new data were analyzed for this summary-type presentation. All background material presented in the figures is available in the references given in the corresponding figure captions.

## REFERENCES

Adams, M., Sterling, A. C., Moore, R. L., and Gary, G. A. (2014). A small-scale eruption leading to a blowout macrospicule jet in an on-disk coronal hole. *Astrophysical Journal* 783, 11. doi:10.1088/0004-637X/783/1/11

Asai, A., Shibata, K., Ishii, T. T., Oka, M., Kataoka, R., Fujiki, K., et al. (2009). Evolution of the anemone AR NOAA 10798 and the related geo-effective flares and CMEs. *Journal of Geophysical Research (Space Physics)* 114, A00A21. doi:10.1029/2008JA013291

Athay, R. G. (1959). The number of spicules in the middle chromosphere. *Astrophysical Journal* 129, 164. doi:10.1086/146603

Baikie, T. K., Sterling, A. C., Moore, R. L., Alexander, A. M., Falconer, D. A., Savcheva, A., et al. (2022). Further Evidence for the Minifilament-Eruption Scenario for Solar Polar Coronal Jets. *arXiv e-prints* , arXiv:2201.08882

Bale, S. D., Badman, S. T., Bonnell, J. W., Bowen, T. A., Burgess, D., Case, A. W., et al. (2019). Highly structured slow solar wind emerging from an equatorial coronal hole. *Nature* 576, 237. doi:10.1038/s41586-019-1818-7

Bale, S. D., Horbury, T. S., Velli, M., Desai, M. I., Halekas, J. S., McManus, M. D., et al. (2021). A Solar Source of Alfvénic Magnetic Field Switchbacks: In Situ Remnants of Magnetic Funnels on Supergranulation Scales. *ApJ* 923, 174. doi:10.3847/1538-4357/ac2d8c

Beckers, J. M. (1968). Solar spicules (invited review paper). *Solar Physics* 3, 367. doi:10.1007/BF00171614

Beckers, J. M. (1972). Solar spicules. *Annual Review of Astronomy and Astrophysics* 10, 73. doi:10.1146/annurev.aa.10.090172.000445

Berghmans, D., Auchère, F., Long, D. M., Soubrié, E., Mierla, M., Zhukov, A. N., et al. (2021). Extreme-UV quiet Sun brightenings observed by the Solar Orbiter/EUI. *Astron. & Astrophys.* 656, L4. doi:10.1051/0004-6361/202140380

Bernasconi, P. N., Rust, D. M., and Hakim, D. (2005). Advanced Automated Solar Filament Detection And Characterization Code: Description, Performance, And Results. *Solar Physics* 228, 97–117. doi:10.1007/s11207-005-2766-y

Brooks, D. H., Warren, H. P., Ugarte-Urra, I., and Winebarger, A. R. (2013). High Spatial Resolution Observations of Loops in the Solar Corona. *ApJ Letters* 772, L19. doi:10.1088/2041-8205/772/2/L19

Canfield, R. C., Reardon, K. P., Leka, K. D., Shibata, K., Yokoyama, T., and Shimojo, M. (1996). H-alpha surges and x-ray jets in ar 7260. *Astrophysical Journal* 464, 1016. doi:10.1086/177389

Chen, P. F. (2011). Coronal Mass Ejections: Models and Their Observational Basis. *Living Reviews in Solar Physics* 8, 1. doi:10.12942/lrsp-2011-1

Cheung, M. C. M., De Pontieu, B., Tarbell, T. D., Fu, Y., Tian, H., Testa, P., et al. (2015). Homologous Helical Jets: Observations By IRIS, SDO, and Hinode and Magnetic Modeling With Data-Driven Simulations. *ApJ* 801, 83. doi:10.1088/0004-637X/801/2/83

Chintzoglou, G., Zhang, J., Cheung, M. C. M., and Kazachenko, M. (2019). The Origin of Major Solar Activity: Collisional Shearing between Nonconjugated Polarities of Multiple Bipoles Emerging within Active Regions. *ApJ* 871, 67. doi:10.3847/1538-4357/aaef30

Cirtain, J. W., Golub, L., Lundquist, L., van Ballegooijen, A., Savcheva, A., Shimojo, M., et al. (2007). Evidence for alfvén waves in solar x-ray jets. *Science* 318, 1580. doi:10.1126/science.1147050

De Pontieu, B., Carlsson, M., Rouppe van der Voort, L. H. M., Rutten, R. J., Hansteen, V. H., and Watanabe, H. (2012). Ubiquitous torsional motions in type ii spicules. *Astrophysical Journal* 752L, 12. doi:10.1088/2041-8205/752/1/L12

De Pontieu, B., Erdélyi, R., and James, S. P. (2004). Solar chromospheric spicules from the leakage of photospheric oscillations and flows. *Nature* 430, 536. doi:10.1038/nature02749

De Pontieu, B., McIntosh, S., Hansteen, V. H., Carlsson, M., Schrijver, C. J., Tarbell, T. D., et al. (2007). A tale of two spicules: The impact of spicules on the magnetic chromosphere. *Publications of the Astronomical Society of Japan* 59, 655. doi:10.1093/pasj/59.sp3.S655

De Pontieu, B., Title, A. M., Lemen, J. R., Kushner, G. D., Akin, D. J., Allard, B., et al. (2014). The interface region imaging spectrograph (iris). *Solar Physics* 289, 2733. doi:10.1007/s11207-014-0485-y

Devi, P., Joshi, B., Chandra, R., Mitra, P. K., Veronig, A. M., and Joshi, R. (2020). Development of a Confined Circular-Cum-Parallel Ribbon Flare and Associated Pre-Flare Activity. *Solar Physics* 295, 75. doi:10.1007/s11207-020-01642-y

Doyle, L., Wyper, P. F., Scullion, E., McLaughlin, J. A., Ramsay, G., and Doyle, J. G. (2019). Observations and 3D Magnetohydrodynamic Modeling of a Confined Helical Jet Launched by a Filament Eruption. *ApJ* 887, 246. doi:10.3847/1538-4357/ab5d39

Drake, J. F., Agapitov, O., Swisdak, M., Badman, S. T., Bale, S. D., Horbury, T. S., et al. (2021). Switchbacks as signatures of magnetic flux ropes generated by interchange reconnection in the corona. *Astron. & Astrophys.* 650, A2. doi:10.1051/0004-6361/202039432

Fargette, N., Lavraud, B., Rouillard, A. P., Réville, V., Bale, S. D., and Kasper, J. (2022). The preferential orientation of magnetic switchbacks and its implications for solar magnetic flux transport. *Astron. & Astrophys.* 663, A109. doi:10.1051/0004-6361/202243537

Fargette, N., Lavraud, B., Rouillard, A. P., Réville, V., Dudok De Wit, T., Froment, C., et al. (2021). Characteristic Scales of Magnetic Switchback Patches Near the Sun and Their Possible Association With Solar Supergranulation and Granulation. *ApJ* 919, 96. doi:10.3847/1538-4357/ac1112

Foukal, P. (2013). *Solar Astrophysics (third, revised edition)* (Weinheim, Germany: WILEY-VCH Verlag GmbH & KGaA)

Golub, L., Deluca, E., Austin, G., Bookbinder, J., Caldwell, D., Cheimets, P., et al. (2007). The x-ray telescope (xrt) for the hinode mission. *Solar Physics* 243, 63. doi:10.1007/s11207-007-0182-1

Golub, L., Krieger, A. S., Silk, J. K., Timothy, A. F., and Vaiana, G. S. (1974). Solar X-Ray Bright Points. *ApJ Letters* 189, L93. doi:10.1086/181472

Handy, B. N., Acton, L. W., Kankelborg, C. C., Wolfson, C. J., Akin, D. J., Bruner, M. E., et al. (1999). The transition region and coronal explorer. *Solar Physics* 187, 229–260. doi:10.1023/A:1005166902804

Hinode Review Team, Khalid, A.-J., Patrick, A., Baker, D., R., B. L., and et al. (2019). Achievements of hinode in the first eleven years. *Publications of the Astronomical Society of Japan* 71, id.R1. doi:10.1093/pasj/psz084

Hirayama, T. (1974). Theoretical model of flares and prominences i evaporating flare model. *Solar Physics* 34, 323. doi:10.1007/BF00153671

Hong, J., Jiang, Y., Zheng, R., Yang, J., Bi, Y., and Yang, B. (2011). A micro coronal mass ejection associated blowout extreme-ultraviolet jet. *Astrophysical Journal* 738L, 20. doi:10.1088/2041-8205/738/2/L20

Huang, M., Z., S., M., Doyle, J. G., and Lamb, D. A. (2012). Coronal hole boundaries at small scales. iv. sot view. magnetic field properties of small-scale transient brightenings in coronal holes. *Astronomy and Astrophysics* 548, 62. doi:10.1051/0004-6361/201220079

Joshi, B., Thalmann, J. K., Mitra, P. K., Chandra, R., and Veronig, A. M. (2017). Observational and model analysis of a two-ribbon flare possibly induced by a neighboring blowout jet. *Astrophysical Journal* 851, 29. doi:10.3847/1538-4357/aa9564

Judge, P. G. and Carlsson, M. (2010). On the solar chromosphere observed at the limb with hinode. *Astrophysical Journal* 719, 469. doi:10.1088/0004-637X/719/1/469

Katsukawa, Y., Berger, T. E., Ichimoto, K., Lites, B. W., Nagata, S., Shimizu, T., et al. (2007). Small-scale jetlike features in penumbral chromospheres. *Science* 318, 1594. doi:10.1126/science.1146046

Kobayashi, K., Cirtain, J., Winebarger, A. R., Korreck, K., Golub, L., Walsh, R. W., et al. (2014). The High-Resolution Coronal Imager (Hi-C). *Solar Physics* 289, 4393–4412. doi:10.1007/s11207-014-0544-4

Kosugi, T., Matsuzaki, K., Sakao, T., Shimizu, T., Sone, Y., Tachikawa, S., et al. (2007). The hinode (solar-b) mission: An overview. *Solar Physics* 243, 3. doi:10.1007/s11207-007-9014-6

Koutchmy, S., Hara, H., Suematsu, Y., and Reardon, K. (1997). Sxr coronal flashes. *Astronomy and Astrophysics* 320L, 33

Kumar, P., Karpen, J. T., Antiochos, S. K., Wyper, P. F., DeVore, C. R., and DeForest, C. E. (2019). Multiwavelength study of equatorial coronal-hole jets. *Astrophysical Journal* 873, 93. doi:10.3847/1538-4357/ab04af

Kumar, P. and Manoharan, P. K. (2013). Eruption of a plasma blob, associated M-class flare, and large-scale extreme-ultraviolet wave observed by SDO. *Astron. & Astrophys.* 553, A109. doi:10.1051/0004-6361/201220283

Lemen, J. R., Title, A. M., Akin, D. J., Boerner, P. F., Chou, C., Drake, J. F., et al. (2012). The atmospheric imaging assembly (aia) on the solar dynamics observatory (sdo). *Solar Physics* 275, 17. doi:10.1007/s11207-011-9776-8

Liu, J., Erdélyi, R., Wang, Y., and Liu, R. (2018). Untwisting jets related to magnetic flux cancellation. *Astrophysical Journal* 852, 10. doi:10.3847/1538-4357/aa992d

Lugaz, N., Downs, C., Shibata, K., Roussev, I. I., Asai, A., and Gombosi, T. I. (2011). Numerical Investigation of a Coronal Mass Ejection from an Anemone Active Region: Reconnection and Deflection of the 2005 August 22 Eruption. *ApJ* 738, 127. doi:10.1088/0004-637X/738/2/127

Lynch, D. K., Beckers, J. M., and Dunn, R. B. (1973). A morphological study of solar spicules. *Solar Physics* 30, 63L. doi:10.1007/BF00156173

Mazumder, R. (2019). Solar Quiet Region Jet by Eruption of Minifilament and Associated Change in Magnetic Flux. *Astronomy Reports* 63, 404–408. doi:10.1134/S1063772919050044

McGlasson, R. A., Panesar, N. K., Sterling, A. C., and Moore, R. L. (2019). Magnetic flux cancellation as the trigger mechanism of solar coronal jets. *ApJ* 882, 16. doi:10.3847/1538-4357/ab2fe3

Moore, R. L., Cirtain, J. W., Sterling, A. C., and Falconer, D. A. (2010). Dichotomy of solar coronal jets: Standard jets and blowout jets. *Astrophysical Journal* 720, 757. doi:10.1088/0004-637X/720/1/757

Moore, R. L., Panesar, N. K., Sterling, A. C., and Tiwari, S. K. (2022). Bipolar Ephemeral Active Regions, Magnetic Flux Cancellation, and Solar Magnetic Explosions. *ApJ* 933, 12. doi:10.3847/1538-4357/ac6181

Moore, R. L., Sterling, A. C., Falconer, D. A., and Robe, D. (2013). The cool component and the dichotomy, lateral expansion, and axial rotation of solar x-ray jets. *Astrophysical Journal* 769, 134. doi:10.1088/0004-637X/769/2/134

Moore, R. L., Sterling, A. C., Hudson, H. S., and Lemen, J. R. (2001). Onset of the magnetic explosion in solar flares and coronal mass ejections. *Astrophysical Journal* 552, 833. doi:10.1086/320559

Moore, R. L., Sterling, R. L., and Falconer, D. A. (2015). Magnetic untwisting in solar jets that go into the outer corona in polar coronal holes. *Astrophysical Journal* 806, 11. doi:10.1088/0004-637X/806/1/11

Muglach, K. (2021). The Photospheric Footpoints of Solar Coronal Hole Jets. *ApJ* 909, 133. doi:10.3847/1538-4357/abd5ad

Mulay, S. M., Del Zanna, G., and Mason, H. (2017a). Cool and hot emission in a recurring active region jet. *Astronomy and Astrophysics* 606, 4. doi:10.1051/0004-6361/201730429

Mulay, S. M., Del Zanna, G., and Mason, H. (2017b). Temperature and density structure of a recurring active region jet. *Astronomy and Astrophysics* 598, 11. doi:10.1051/0004-6361/201628796

Mulay, S. M., Tripathi, D. T., Del Zanna, G., and Mason, H. (2016). Multiwavelength study of 20 jets that emanate from the periphery of active regions. *Astronomy and Astrophysics* 589, A79. doi:10.1051/0004-6361/201527473

Neugebauer, M. and Sterling, A. C. (2021). Relation of Microstreams in the Polar Solar Wind to Switchbacks and Coronal X-Ray Jets. *ApJ Letters* 920, L31. doi:10.3847/2041-8213/ac2945

Nishizuka, N., Shimizu, M., Nakamura, T., Otsuji, K., Okamoto, T. J., Katsukawa, Y., et al. (2008). Giant chromospheric anemone jet observed with hinode and comparison with magnetohydrodynamic simulations: Evidence of propagating alfvén waves and magnetic reconnection. *Astrophysical Journal* 683, 83. doi:10.1086/591445

Nisticò, G., Bothmer, V., Patsourakos, S., and Zimbardo, G. (2009). Characteristics of euv coronal jets observed with *stereo*/secchi. *Solar Physics* 259, 87. doi:10.1007/s11207-009-9424-8

Nisticò, G., Bothmer, V., Patsourakos, S., and Zimbardo, G. (2010). Observational features of equatorial coronal hole jets. *Annales Geophysicae* 28, 687. doi:10.5194/angeo-28-687-2010

Nisticò, G., Patsourakos, S., Bothmer, V., and Zimbardo, G. (2011). Determination of temperature maps of EUV coronal hole jets. *Advances in Space Research* 48, 1490–1498. doi:10.1016/j.asr.2011.07.003

Owens, M., Lockwood, M., Macneil, A., and Stansby, D. (2020). Signatures of Coronal Loop Opening via Interchange Reconnection in the Slow Solar Wind at 1 AU. *Solar Physics* 295, 37. doi:10.1007/s11207-020-01601-7

Panesar, N. K., Sterling, A. C., and Moore, R. L. (2016a). Homologous jet-driven coronal mass ejections from solar active region 12192. *Astrophysical Journal* 822L, 7. doi:10.3847/2041-8205/822/2/L23

Panesar, N. K., Sterling, A. C., and Moore, R. L. (2017). Magnetic flux cancellation as the origin of solar quiet-region pre-jet minifilaments. *Astrophysical Journal* 844, 131. doi:10.3847/1538-4357/aa7b77

Panesar, N. K., Sterling, A. C., and Moore, R. L. (2018a). Magnetic flux cancelation as the trigger of solar coronal jets in coronal holes. *Astrophysical Journal* 853, 189. doi:10.3847/1538-4357/aaa3e9

Panesar, N. K., Sterling, A. C., Moore, R. L., and Chakrapani, P. (2016b). Magnetic flux cancelation as the trigger of solar quiet-region coronal jets. *Astrophysical Journal* 832L, 7. doi:10.3847/2041-8205/832/1/L7

Panesar, N. K., Sterling, A. C., Moore, R. L., Tiwari, r. S. K., De Pontieu, B., and Norton, A. A. (2018b). Iris and sdo observations of solar jetlets resulting from network-edge flux cancelation. *Astrophysical Journal* 868L, 27. doi:10.3847/2041-8213/aaef37

Panesar, N. K., Sterling, A. C., Moore, R. L., Winebarger, A. R., Tiwari, S. K., Savage, S. L., et al. (2019). Hi-C 2.1 Observations of Jetlet-like Events at Edges of Solar Magnetic Network Lanes. *ApJ Letters* 887, L8. doi:10.3847/2041-8213/ab594a

Panesar, N. K., Tiwari, S. K., Berghmans, D., Cheung, M. C. M., Müller, D., Auchere, F., et al. (2021). The Magnetic Origin of Solar Campfires. *ApJ Letters* 921, L20. doi:10.3847/2041-8213/ac3007

Panesar, N. K., Tiwari, S. K., Moore, R. L., Sterling, A. C., and De Pontieu, B. (2022). Genesis and Coronal-jet-generating Eruption of a Solar Minifilament Captured by IRIS Slit-raster Spectra. *ApJ* 939, 25. doi:10.3847/1538-4357/ac8d65

Paraschiv, A. R., Bemporad, A., and Sterling, A. C. (2015). Physical properties of solar polar jets. *A statistical study with Hinode XRT data, Astronomy and Astrophysics* 579, 96. doi:10.1051/0004-6361/201525671

Paraschiv, A. R., Donea, A. C., and Judge, P. G. (2022). Thermal and Non-thermal Properties of Active Region Recurrent Coronal Jets. *ApJ* 935, 172. doi:10.3847/1538-4357/ac80fb

Pasachoff, J. M., Noyes, R. W., and Beckers, J. M. (1968). Spectral observations of spicules at two heights in the solar chromosphere. *Solar Physics* 5, 131. doi:10.1007/BF00147962

Pike, C. D. and Mason, H. E. (1998). Rotating transition region features observed with the soho coronal diagnostic spectrometer. *Solar Physics* 182, 333. doi:10.1023/A:1005065704108

Poletto, G. (2015). Solar coronal plumes. *Living Reviews in Solar Physics* 12, 7. doi:10.1007/lrsp-2015-7

Pucci, S., Poletto, G., Sterling, A. C., and Romoli, M. (2013). Physical parameters of standard and blowout jets. *Astrophysical Journal* 776, 16. doi:10.1088/0004-637X/776/1/16

Rachmeler, L. A., Winebarger, A. R., Savage, S. L., Golub, L., Kobayashi, K., Vigil, G. D., et al. (2019). The High-Resolution Coronal Imager, Flight 2.1. *Solar Physics* 294, 174. doi:10.1007/s11207-019-1551-2

Raouafi, N. E., Patsourakos, S., Pariat, E., Young, P. R., Sterling, A. C., Savcheva, A., et al. (2016). Solar coronal jets: Observations, theory, and modeling. *Space Science Reviews* 201, 1. doi:10.1007/s11214-016-0260-5

Raouafi, N. E. and Stenborg, G. (2014). Role of transients in the sustainability of solar coronal plumes. *Astrophysical Journal* 787, 118. doi:10.1088/0004-637X/787/2/118

Ruan, G., Schmieder, B., Masson, S., Mein, P., Mein, N., Aulanier, G., et al. (2019). Bidirectional Reconnection Outflows in an Active Region. *ApJ* 883, 52. doi:10.3847/1538-4357/ab3657

Samanta, T., Tian, H., Yurchyshyn, V., Peter, H., Cao, W., Sterling, A., et al. (2019). Generation of solar spicules and subsequent atmospheric heating. *Science* 366, 890. doi:10.1126/science.aaw2796

Savcheva, A., Cirtain, J., Deluca, E. E., Lundquist, L. L., Golub, L., Weber, M., et al. (2007). A study of polar jet parameters based on hinode xrt observations. *Publications of the Astronomical Society of Japan* 59, 771. doi:10.1093/pasj/59.sp3.S771

Scherrer, P. H., Schou, J., Bush, R. I., Kosovichev, A. G., Bogart, R. S., Hoeksema, J. T., et al. (2012). The helioseismic and magnetic imager (hmi) investigation for the solar dynamics observatory (sdo). *Solar Physics* 275, 207. doi:10.1007/s11207-011-9834-2

Schmieder, B. (2022). Solar jets: SDO and IRIS observations in the perspective of new MHD simulations. *arXiv e-prints* , arXiv:2201.11541

Schmieder, B., Joshi, R., and Chandra, R. (2022). Solar jets observed with the Interface Region Imaging Spectrograph (IRIS). *Advances in Space Research* 70, 1580–1591. doi:10.1016/j.asr.2021.12.013

Schwadron, N. A. and McComas, D. J. (2021). Switchbacks Explained: Super-Parker Fields—The Other Side of the Sub-Parker Spiral. *ApJ* 909, 95. doi:10.3847/1538-4357/abd4e6

Shen, Y. (2021). Observation and modelling of solar jets. *Proceedings of the Royal Society of London Series A* 477, 217. doi:10.1098/rspa.2020.0217

Shen, Y., Liu, Y., Su, J., and Deng, Y. (2012). On a coronal blowout jet: the first observation of a simultaneously produced bubble-like cme and a jet-like cme in a solar event. *Astrophysical Journal* 745, 164. doi:10.1088/0004-637X/745/2/164

Shibata, K., Ishido, Y., Acton, L. W., Strong, K. T., Hirayama, T., Uchida, Y., et al. (1992). Observations of x-ray jets with the yohkoh soft x-ray telescope. *Publications of the Astronomical Society of Japan* 44, L173

Shibata, K. and Magara, T. (2011). Solar flares: Magnetohydrodynamic processes. *LRSP* 8, 6

Shibata, K., Masuda, S., Shimojo, M., Hara, H., Yokoyama, T., Tsuneta, S., et al. (1995). Hot-Plasma Ejections Associated with Compact-Loop Solar Flares. *ApJ Letters* 451, L83. doi:10.1086/309688

Shibata, K., Nakamura, T., Matsumoto, T., Otsuji, K., Okamoto, T. J., Nishizuka, N., et al. (2007). Chromospheric anemone jets as evidence of ubiquitous reconnection. *Science* 318, 1591. doi:10.1126/science.1146708

Shibata, K. and Uchida, Y. (1986). A magnetodynamic mechanism for the formation of astrophysical jets. ii - dynamical processes in the accretion of magnetized mass in rotation. *Solar Physics* 178, 379

Shimojo, M., Hashimoto, S., Shibata, K., Hirayama, T., Hudson, H. S., and Acton, L. W. (1996). Statistical study of solar x-ray jets observed with the yohkoh soft x-ray telescope. *Publications of the Astronomical Society of Japan* 48, 123. doi:10.1093/pasj/48.1.123

Shimojo, M. and Shibata, K. (2000). Physical parameters of solar x-ray jets. *Astrophysical Journal* 542, 1100. doi:10.1086/317024

Solanki, R., Srivastava, A. K., Rao, Y. K., and Dwivedi, B. N. (2019). Twin cme launched by a blowout jet originated from the eruption of a quiet-sun mini-filament. *Solar Physics* 294, 68. doi:10.1007/s11207-019-1453-3

Sterling, A. C. (2000). Solar spicules: A review of recent models and targets for future observations - (invited review). *Solar Physics* 196, 79. doi:10.1023/A:1005213923962

Sterling, A. C. (2018). Coronal Jets, and the Jet-CME Connection. In *Journal of Physics Conference Series*. vol. 1100 of *Journal of Physics Conference Series*, 012024. doi:10.1088/1742-6596/1100/1/012024

Sterling, A. C. (2021). Fine-Scale Features of the Sun's Atmosphere: Spicules and Jets. In *Solar Physics and Solar Wind*, eds. N. E. Raouafi and A. Vourlidas. vol. 1, 221. doi:10.1002/9781119815600.ch6

Sterling, A. C. and Moore, R. L. (2001). Eit crinkles as evidence for the breakout model of solar eruptions. *Astrophysical Journal* 560, 1045. doi:10.1086/322241

Sterling, A. C. and Moore, R. L. (2001). Internal and external reconnection in a series of homologous solar flares. *JGR* 106, 25227–25238. doi:10.1029/2000JA004001

Sterling, A. C. and Moore, R. L. (2016). A microfilament-eruption mechanism for solar spicules. *Astrophysical Journal* 828, L9. doi:10.3847/2041-8205/828/1/L9

Sterling, A. C. and Moore, R. L. (2020). Coronal-jet-producing Minifilament Eruptions as a Possible Source of Parker Solar Probe Switchbacks. *ApJ Letters* 896, L18. doi:10.3847/2041-8213/ab96be

Sterling, A. C. and Moore, R. L. (in press 2022). Future High-Resolution and High-Cadence Observations for Unraveling Eruptive Solar Features. *Bullet. Amer. Astron. Soc.*

Sterling, A. C., Moore, R. L., Falconer, D. A., and Adams, M. (2015). Small-scale filament eruptions as the driver of x-ray jets in solar coronal holes. *Nature* 523, 437. doi:10.1038/nature14556

Sterling, A. C., Moore, R. L., Falconer, D. A., Panesar, N. K., Akiyama, S., Yashiro, S., et al. (2016). Minifilament eruptions that drive coronal jets in a solar active region. *Astrophysical Journal* 821, 100. doi:10.3847/0004-637X/821/2/100

Sterling, A. C., Moore, R. L., Falconer, D. A., Panesar, N. K., and Martinez, F. (2017). Solar active region coronal jets. ii. triggering and evolution of violent jets. *Astrophysical Journal* 844, 28. doi:10.3847/1538-4357/aa7945

Sterling, A. C., Moore, R. L., and Panesar, N. K. (2018). Magnetic flux cancelation as the buildup and trigger mechanism for cme-producing eruptions in two small active regions. *Astrophysical Journal* 864, 68. doi:10.3847/1538-4357/aad550

Sterling, A. C., Moore, R. L., and Panesar, N. K. (2022). Another Look at Erupting Minifilaments at the Base of Solar X-Ray Polar Coronal "Standard" and "Blowout" Jets. *ApJ* 927, 127. doi:10.3847/1538-4357/ac473f

Sterling, A. C., Moore, R. L., Panesar, N. K., Reardon, K. P., Molnar, M., Rachmeler, L. A., et al. (2020a). Hi-C 2.1 Observations of Small-scale Miniature-filament-eruption-like Cool Ejections in an Active Region Plage. *ApJ* 889, 187. doi:10.3847/1538-4357/ab5dcc

Sterling, A. C., Moore, R. L., Qiu, J., and Wang, H. (2001). H$\alpha$ Proxies for EIT Crinkles: Further Evidence for Preflare "Breakout"-Type Activity in an Ejective Solar Eruption. *ApJ* 561, 1116–1126. doi:10.1086/323374

Sterling, A. C., Moore, R. L., Samanta, T., and Yurchyshyn, V. (2020b). Possible Production of Solar Spicules by Microfilament Eruptions. *ApJ Letters* 893, L45. doi:10.3847/2041-8213/ab86a5

Tandberg-Hanssen, E. (1995). *The nature of solar prominences*, vol. 199 (Kluwer Academic Publishers). doi:10.1007/978-94-017-3396-0

Tian, H., DeLuca, E. E., Cranmer, S. R., De Pontieu, B., Peter, H., Martínez-Sykora, J., et al. (2014). Prevalence of small-scale jets from the networks of the solar transition region and chromosphere. *Science* 346. doi:10.1126/science.1255711

Tiwari, S. K., Moore, R. L., De Pontieu, B., Tarbell, T. D., Panesar, N. K., Winebarger, A. R., et al. (2018). Evidence of twisting and mixed-polarity solar photospheric magnetic field in large penumbral jets: Iris and hinode observations. *Astrophysical Journal* 869, 147. doi:10.3847/1538-4357/aaf1b8

Tiwari, S. K., Moore, R. L., Winebarger, A. R., and Alpert, S. E. (2016). Transition-region/coronal signatures and magnetic setting of sunspot penumbral jets: Hinode (sot/fg), hi-c, and sdo/aia observations. *Astrophysical Journal* 816, 92. doi:10.3847/0004-637X/816/2/92

Tiwari, S. K., Panesar, N. K., Moore, R. L., De Pontieu, B., Winebarger, A. R., Golub, L., et al. (2019). Fine-scale Explosive Energy Release at Sites of Prospective Magnetic Flux Cancellation in the Core of the Solar Active Region Observed by Hi-C 2.1, IRIS, and SDO. *ApJ* 887, 56. doi:10.3847/1538-4357/ab54c1

Tiwari, S. K., van Noort, M., Lagg, A., and Solanki, S. K. (2013). Structure of sunspot penumbral filaments: a remarkable uniformity of properties. *Astron. & Astrophys.* 557, A25. doi:10.1051/0004-6361/201321391

Tsiropoula, G., Tziotziou, K., Kontogiannis, I., Madjarska, M. S., Doyle, J. G., and Suematsu, Y. (2012). Solar fine-scale structures. i. spicules and other small-scale, jet-like events at the chromospheric level: Observations and physical parameters. *Space Science Reviews* 169, 181. doi:10.1007/s11214-012-9920-2

Tsuneta, S., Acton, L., Bruner, M., Lemen, J., Brown, W., Caravalho, R., et al. (1991). The soft x-ray telescope for the solar-a mission. *Solar Physics* 136, 37. doi:10.1007/BF00151694

van Ballegooijen, A. A. and Martens, P. C. H. (1989). Formation and eruption of solar prominences. *Astrophysical Journal* 343, 971. doi:10.1086/167766

Wang, Y.-M., Sheeley, N. R., Jr., Socker, G., D., Howard, R. A., et al. (1998). Observations of correlated white-light and extreme-ultraviolet jets from polar coronal holes. *Astrophysical Journal* 508, 899. doi:10.1086/306450

Wyper, P. F., Antiochos, S. K., and DeVore, C. R. (2017). A universal model for solar eruptions. *Nature* 544, 452. doi:10.1038/nature22050

Wyper, P. F., DeVore, C. R., and Antiochos, S. K. (2018a). Breakout model for solar coronal jets with filaments. *Astrophysical Journal* 852, 98. doi:10.3847/1538-4357/aa9ffc

Wyper, P. F., DeVore, C. R., and Antiochos, S. K. (2019). Numerical simulation of helical jets at active region peripheries. *Month. Not. Royal Astro. Soc.* 490, 3679–3690. doi:10.1093/mnras/stz2674

Wyper, P. F., DeVore, C. R., Karpen, J. T., Antiochos, S. K., and Yeates, A. R. (2018b). A model for coronal hole bright points and jets due to moving magnetic elements. *Astrophysical Journal* 864, 165. doi:10.3847/1538-4357/aad9f7

Yang, B., Yang, J., Bi, Y., Xu, Z., Hong, J., Li, H., et al. (2019). Recurrent Two-sided Loop Jets Caused By Magnetic Reconnection between Erupting Minifilaments and a nearby Large Filament. *ApJ* 887, 220. doi:10.3847/1538-4357/ab557e

Yashiro, S., Gopalswamy, N., Michalek, G., St. Cyr, O. C., Plunkett, S. P., Rich, N. B., et al. (2004). A catalog of white light coronal mass ejections observed by the SOHO spacecraft. *Journal of Geophysical Research (Space Physics)* 109, A07105. doi:10.1029/2003JA010282

Yokoyama, T. and Shibata, K. (1995). Magnetic reconnection as the origin of x-ray jets and h$\alpha$ surges on the sun. *Nature* 375, 42. doi:10.1038/375042a0

Yu, H.-S., Jackson, B. V., Buffington, A., Hick, P. P., Shimojo, M., and Sako, N. (2014). The three-dimensional analysis of hinode polar jets using images from lasco c2, the stereo cor2 coronagraphs, and smei. *Astrophysical Journal* 784, 166. doi:10.1088/0004-637X/784/2/166

Yu, H.-S., Jackson, B. V., Yang, Y. H., Chen, N. H., Buffington, A., and Hick, P. P. (2016). A 17 june 2011 polar jet and its presence in the background solar wind. *Journal of Geophysical Research: Space Physics* 121, 4985. doi:10.1002/2016JA022503

Zank, G. P., Nakanotani, M., Zhao, L. L., Adhikari, L., and Kasper, J. (2020). The Origin of Switchbacks in the Solar Corona: Linear Theory. *ApJ* 903, 1. doi:10.3847/1538-4357/abb828

## 6 APPENDIX

Here we summarize information about selected jet-like features in the solar atmosphere, and state how SEIM will enhance our understanding of the mechanism(s) driving these features. This listing is not intended to be exhaustive.

For each entry we provide the following. (1) The chief references for the numbers listed in the given entry. Because many authors and observers measure parameters in different ways, it is difficult to summarize accurately all of the values outside of an extensive review article. Therefore we list the sources used for presenting the specific values listed in this Appendix. (2) Wavelength: the principle wavelength regime where the features are observed. (3) Appearance: The general defining characteristic appearance of the features. (4) Size: Approximate characteristic size for the indicated dimension(s) and/or portion(s) of the features. (5) Lifetimes: typical durations of the events. (6) Energies. (7) Locations: Additional information of where on the Sun the features are typically observed. (8) SEIM Objectives: Some of the unresolved aspects of the features and/or their production mechanism to which SEIM can contribute improved understanding.

**Coronal jets:** *Chief references for following parameters*: Savcheva et al. (2007); Panesar et al. (2016b); Sterling et al. (2018). *Wavelength:* mainly EUV and SXRs, but can have manifestations at other wavelengths too. *Appearance:* Has a spire that grows to be long and narrow, emanating from a base region that is typically bright in SXRs. *Size*: spire; typically ∼10,000 × 50,000 km in SXRs; base: up to a few $\times 10^4$ km in width in EUV. *Lifetimes*: tens of minutes. *Energies*: $\sim 10^{26}$—$10^{29}$ erg. *Locations*: Exist in various solar regions, including coronal holes (sometimes called "coronal hole jets"), quiet Sun ("quiet Sun jets"), and the edges of active regions ("active region jets"). *SEIM Objectives*: Many coronal jets result from eruptions of minifilaments, where the eruptions can be either confined or ejective, and where the eruptions are often observed to result from magnetic flux cancelation. A localized brightening (called the jet bright point or the "JBP") usually forms on one edge of the base of the coronal jet, below the erupting minifilament. The JBP is argued to be a small-scale version of a typical solar flare arcade that forms below a typical erupting filament. Many coronal jets show spire rotations, consistent with magnetic untwisting. See main text and Figure 2 for more details on the proposed mechanism. SEIM, in conjunction with other instruments, will test further this idea for the production of coronal jets, and investigate what percentage of coronal jets are consistent with this production mechanism, and how many might be due to a different mechanism.

**Surges**: *Chief references for following parameters*: Foukal (2013); Moore et al. (2010, 2013); Sterling et al. (2016); Yokoyama and Shibata (1995); Tandberg-Hanssen (1995). *Wavelength*: primarily chromospheric lines, UV, and EUV (304 Å). *Appearance*: traditionally seen as violent expulsions of chromospheric material from bipolar footpoints in active regions, with bright flare-like base brightenings. *Size*: maximum length: up to, but generally much less than, (1–2) $\times 10^5$ km. *Lifetimes*: few tens of minutes. *Energies*: $\lesssim 10^{30}$ erg. *Locations*: Traditionally in active regions. *SEIM Objectives*: Although traditionally defined as an active region phenomenon, surge-like events are seen in quieter regions also. EUV 304 Å surge-like ejections are often seen coincident with coronal jets, even in coronal holes. SEIM will observe coronal-jet locations both in and outside of active regions, and determine whether they are the same basic physical phenomenon. The connection between the surge-like cool-plasma ejecta and the hotter coronal-jet spires that they accompany can be explained in different ways, depending upon the mechanism assumed to be creating the coronal jets. We expect SEIM to see the cool surge material in absorption, and also the hotter bright base of many surges; these observations, in conjunction with other instruments, will help determine

which idea for coronal-jet production most closely aligns with observations of surges and surge-like features.

**Jetlets**: *Chief references for following parameters*: Raouafi and Stenborg (2014); Panesar et al. (2018b); Panesar et al. (2019). *Wavelength*: EUV, mainly 171, 172, and 193 Å; UV. *Appearance*: spire that grows to be long and narrow, similar to coronal jets but smaller in size. First identified at the base of plumes, but later found to be common more generally at the edges of the magnetic network. *Size*: maximum length: ∼10,000—35,000 km in AIA 171 Å, ∼7000—25,000 km in *IRIS* UV; width: ∼1000—7000 km, in both AIA 171 Å and *IRIS* UV. *Lifetimes*: tens of seconds to ∼5 min. *Energies*: Not provided in listed sources. *Locations*: Magnetic network. *SEIM Objectives*: There is currently some evidence that jetlets are small-scale coronal jets, but this is not yet established. SEIM, in conjunction with other instruments, will continue to investigate whether they have properties analogous to coronal jets, UV network jets, and possibly other features.

**UV Network Jets**: *Chief references for following parameters*: Tian et al. (2014). *Wavelength*: UV. *Appearance*: Spire that grows to be long and narrow, similar to coronal jets but smaller in size. *Size*: length: ∼4000—10,000 km; width: ∼300 km. *Lifetimes*: 20—80 s. *Energies*: Energy of individual event not provide in Tian et al. (2014), but likely $\sim 10^{24}$—$10^{26}$ erg, given that a typical one is slightly larger than a typical spicule. *Locations*: Magnetic network. *SEIM Objectives*: It is unknown whether these features are small jetlets, relatively large spicules, or something different from both. SEIM will not observe in UV, but in conjunction with other instruments (IRIS, or a similar instrument) SEIM will investigate whether these features have properties analogous to coronal jets and/or jetlets, including brightenings detectable in EUV at their bases.

**Spicules**: *Chief references for following parameters*: Beckers (1968); Sterling (2000); De Pontieu et al. (2007); Hinode Review Team et al. (2019), T. Pereira subsection; Samanta et al. (2019). *Wavelength*: Traditionally seen in chromospheric lines. Similar features are seen at UV wavelengths too, at least some of which are components of the chromospheric features. *Appearance*: chromospheric-material spire that grows to be long and narrow. *Size*: maximum length: $\lesssim$5000 km; width, ∼(1—few) $\times 10^2$ km. *Lifetimes*: tens of seconds to a few minutes. *Energies*: $\lesssim 10^{25}$ erg. *Locations*: Magnetic network. *SEIM Objectives*: It has been suggested that some spicules might be scaled-down versions of coronal jets (Sterling and Moore, 2016; Sterling et al., 2020b). If this is the case, then some such spicules might be expected to have brightenings at their bases, some of which might be visible in EUV. SEIM will look for such brightenings, and compare with similar observations at the bases of coronal jets, jetlets, and similar features.

**Penumbral jets**: *Chief references for following parameters*: Katsukawa et al. (2007); Tiwari et al. (2016, 2018). *Wavelength*: Until now, most observations are from *Hinode*/Solar Optical Telescope (SOT) Ca II H images and *IRIS* UV data. *Appearance*: transient, long and very narrow, faint features seen in sunspot penumbra at high spatial resolution. *Size*: maximum length: typically 1000—4000 km, but some extend up to 10,000 km; width, $\lesssim$400—600 km. *Lifetimes*: $<$1 min. *Locations*: Sunspot penumbrae. *SEIM Objectives*: Tiwari et al. (2018) suggest that penumbral jets might form from magnetic processes similar to those suspected of causing coronal jets. SEIM will likely not observe penumbral jets directly due to their suspected low temperature (i.e., little or no emission in coronal EUV is expected from them). But a better characterization of properties of coronal jets and similar features with SEIM, in conjunction with other instruments, will provide fresh data with which to compare penumbral filaments, to help ascertain how closely their production mechanism might resemble that of coronal jets.

**Campfires**: *Chief references for following parameters*: Panesar et al. (2021); Berghmans et al. (2021) *Wavelength*: Until now, EUV images from SO/EUI 174 Å, and from AIA; and magentograms from HMI. *Appearance*: small-scale, short-lived coronal brightenings, that can appear as loop-like, dot-like, jet-like, or complex structures. *Size*: length: $\sim$5000 km; width: $\sim$1500 km. *Lifetimes*: $\sim$1—60 min; most $<$10 min. *Locations*: So far only studied in quiet Sun and polar regions, but observations have so far been limited. They occur at the the edge of magnetic network lanes. *SEIM Objectives*: Panesar et al. (2021) find campfires to have similarities to coronal jets or pre-coronal-jet minifilament regions, in that they occur on magnetic neutral lines and most contain transient cool-plasma structures. SEIM observations, in conjunction with other instruments, will clarify whether some or all campfires are powered in the manner in which coronal jets and pre-coronal-jet X-ray-bright locations are powered. More generally, some campfires appear similar to small-scale brightenings called *X-ray bright points* (XBPs) and/or X-ray bright-point flares, that have been observed since the 1970s (Golub et al., 1974), with the campfires perhaps being smaller-scale and less-energetic versions of XBP brightenings; and some of them may be small-scale coronal jets. SEIM, along with complementary instruments, will be able to observe both XBPs and campfires, and of course coronal jets, providing information to determine whether these features operate by the same or different physical mechanisms.

## FIGURES

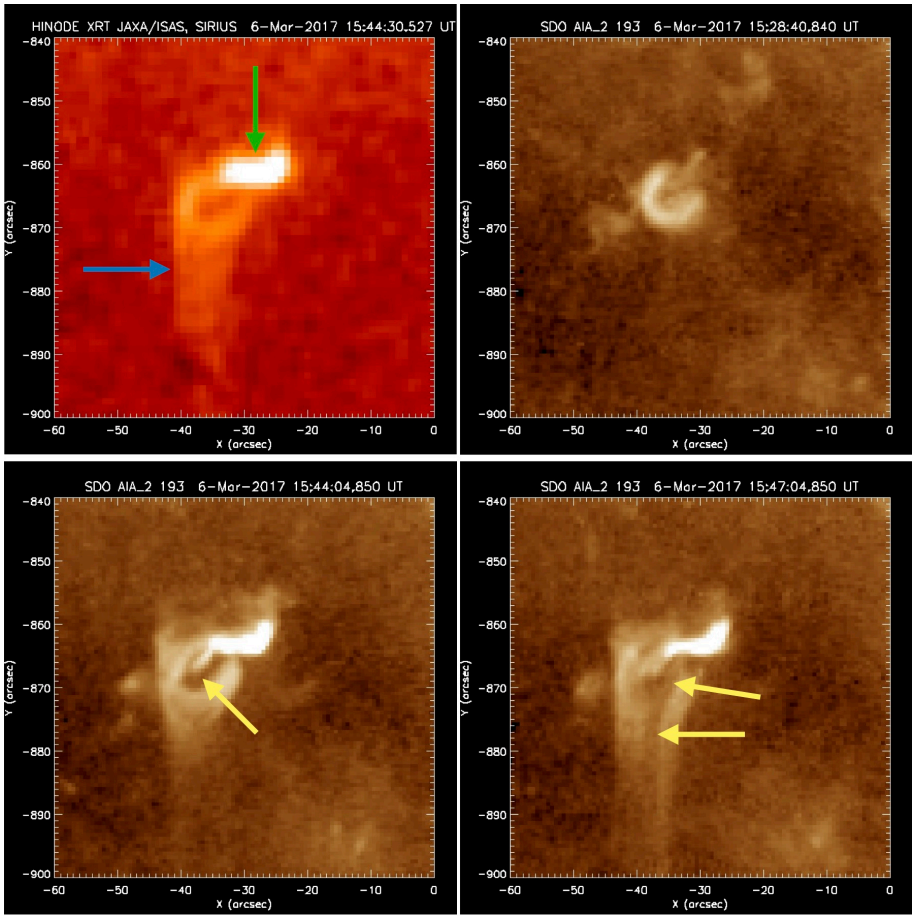


**Figure 1.** Example of a coronal jet, occurring on 2017 March 6. (a) *Hinode*/XRT soft X-ray image of the coronal-jet spire (blue arrow) and the jet bright point ("JBP") brightening in the coronal-jet's base (green arrow). North is upward and west is to the right in this and all solar images in this paper. This coronal jet is in the south polar region, and hence the spire is pointing downward.

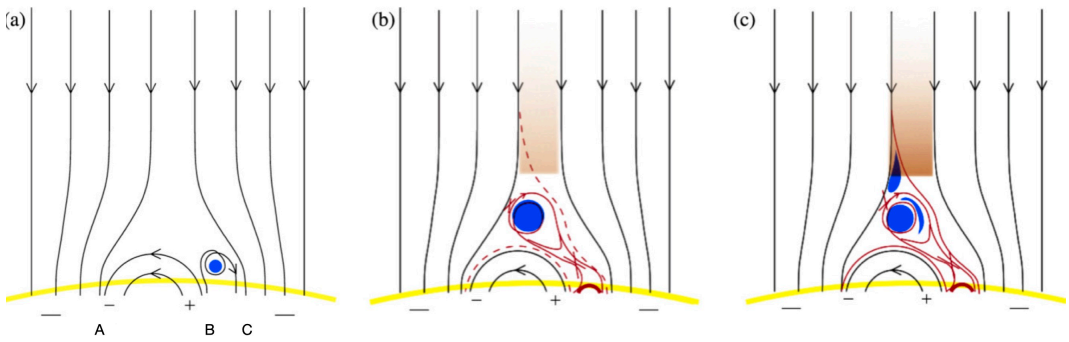


**Figure 2.** Schematic showing the minifilament-eruption mechanism for coronal jets, from Sterling et al. (2015) (this slightly modified version of the original figure appeared in Sterling et al., 2018). This is a two-dimensional cross-sectional cut of the jetting region, with the yellow curve representing the Sun's limb. Black lines represent magnetic field lines prior to reconnection, with the arrow heads and the "+" and "-" signs indicating polarities. Red lines indicate reconnected field lines, with the dotted red lines indicating that the field lines are newly reconnected. The blue circle indicates cool minifilament material, with the circular field surrounding it being the minifilament's field. Panel (a) shows the situation prior to eruption. "A," "B," and "C" indicate locations for reference. In (b) the minifiament's field is erupting, carrying with it the cool minifilament material. Red X-es show reconnections, with the one below the erupting minifilament being flare-like reconnection (called "internal" reconnection, being internal to the erupting flux-tube's lobe field; Sterling et al., 2015) resulting in the jet bright point (JBP), represented by the thick-red simicircle between the B and C locations. The reconnection in front of (to the left and slightly above the center of) the erupting minifilament ("external" reconnection) results in new open field, along which heated plasma flows to form the coronal jet's spire (shaded region). This reconnection also adds new heated closed field above the magnetic lobe between locations A and B. In (c) the higher-height reconnection has proceeded enough that some of the cool minifilament material is flowing out onto the spire on newly reconnected open field.

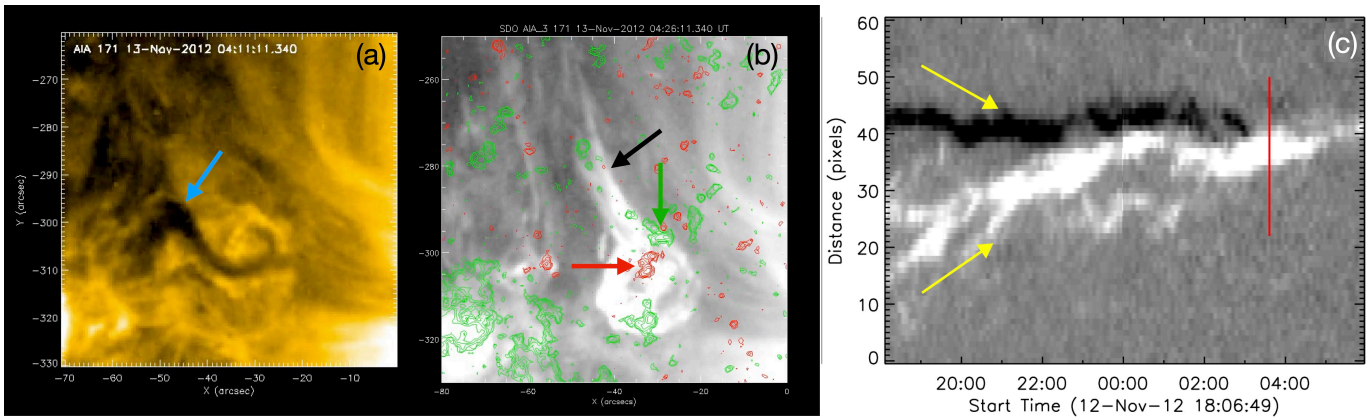


**Figure 3.** Observations of a coronal jet originating from an on-disk location, on 2012 November 13, from Panesar et al. (2016b). Panel (a) is an *SDO*/AIA 193 Å image, showing a minifilament (blue arrow) starting to erupt to produce the coronal jet. Panel (b) shows an AIA 193 Å image (grey scale) 15 minutes later, where the minifilament has erupted and generated the coronal jet, with the black arrow pointing to the spire. Overlaid is magnetic flux from an *SDO*/HMI magnetogram, with red/green contours indicating positive/negative polarities. Red and green arrows point to two polarity elements highlighted in the next panel. Panel (c) shows the time evolution of those positive-polarity (white) and negative-polarity (black) fluxes in a time-distance map, with the vertical red line indicating the time of coronal-jet occurrence. This shows the polarities converging and undergoing cancelation near the time of the coronal-jet's onset.

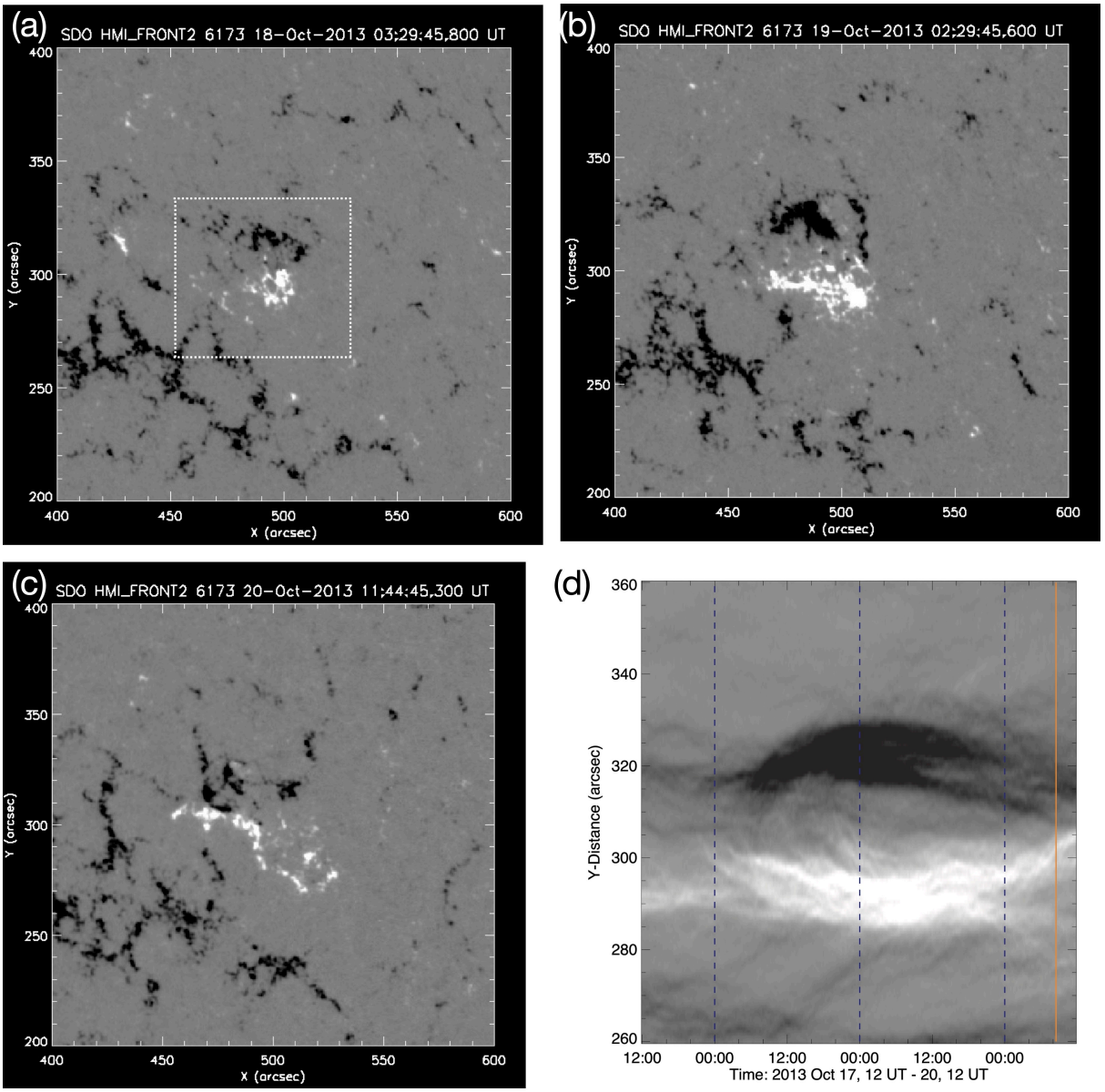


**Figure 4.** *SDO*/HMI magnetograms showing the evolution of a small-sized active region, NOAA AR 11868, which started emerging on 2013 October 16, and which produced a C-class flare and expelled a CME four days later on October 20. (a) The boxed region shows the emerging bipolar region about two days after the start of emergence. Black/white indicate negative/positive magnetic polarities. (b) The main negative and positive patches of the emerging region continue to grow and spread apart. (c) Portions of the opposite-polarity patches have converged on each other, and mangnetic cancelation is occurring between them. (d) A time-distance plot showing evolution of the two polarity patches of the region. This plot is formed by summing fluxes in the horizontal direction across the box in (a), and the y-axis of this panel is a sub-portion of the y-axis of panels (a—c). (From Sterling et al. 2018.)

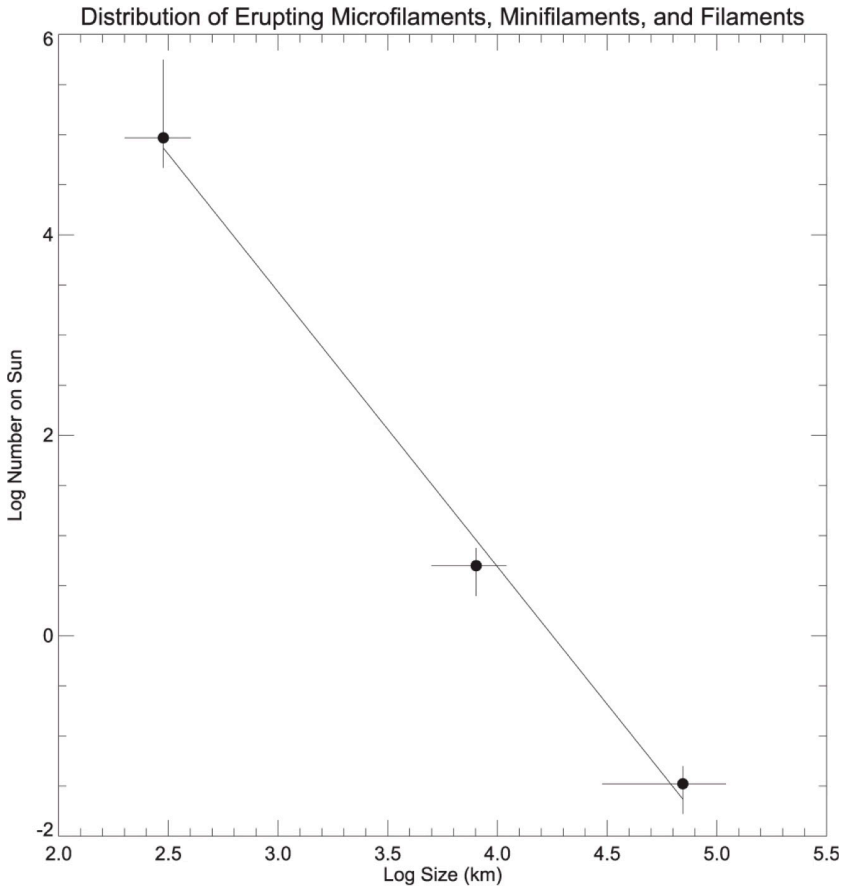


**Figure 5.** Plot showing the instantaneous number distribution of filament-like eruptive events on the Sun, where those eruptions plausibly all operate by the same general eruptive mechanism as that for coronal jets pictured in Fig. 2. The horizontal axis is the size of the erupting cool-material feature, and the vertical axis shows an estimate of the number of eruptions of those features occurring on the Sun at any given time. There are only three points plotted. The right-most point represents large-scale eruptions of typical-sized filaments that produce solar flares, and CMEs in the case of ejective eruptions. The middle point represents coronal jets, such as shown in Figs. 1 and 3, and which are made by minifilament eruptions as depicted in Fig. 2. The leftmost point is for speculative "erupting microfilaments" (erupting microfilament-carrying flux ropes) of the size scale of spicules, and which might produce spicules or spicule-like features in the manner of Fig. 2. "Error" bars represent uncertainties in the observational parameters. This plot demonstrates the plausibility that spicules might fit on the same power-law distribution as large-scale eruptions and the minifilament eruptions that make jets, but much more evidence is required before a firm conclusion can be make regarding whether some or most spicules are generated in a manner analogous to how coronal jets are made. This plot is from Sterling and Moore (2016); see that paper for further details.

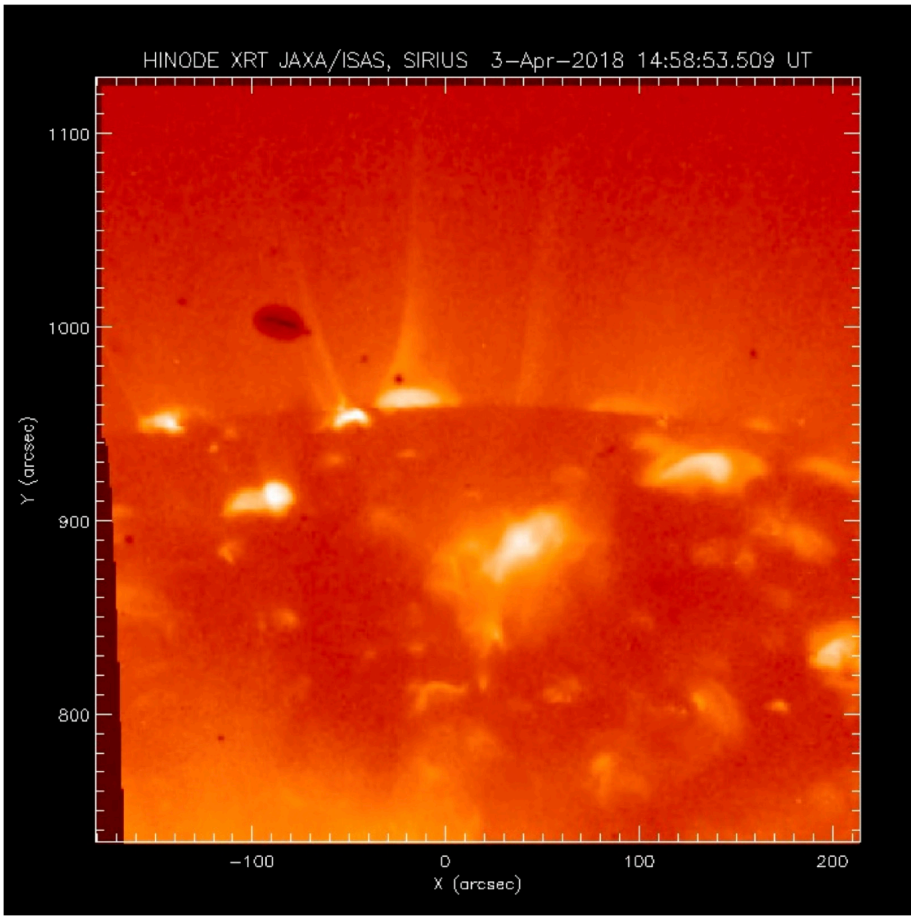


**Figure 6.** *Hinode*/XRT image in SXRs (from Sterling et al., 2022) of the northern polar coronal hole region, showing several coronal jets. The field of view (FOV) here is $6'.67 \times 6'.67$. This is a little larger than the minimum FOV ($6'.0 \times 6'.0$) that would be desired for the suggested SEIM mission. (The dark oval near (-100,1000) and similar smaller dark spots are imaging artifacts.)